Nuclear-radiation detectors based on inorganic scintillators

Yu. K. Akimov
Joint Institute for Nuclear Research, Dubna

Fiz. Elem. Chastits At. Yadra **25**, 229–284 (January–February 1994)

The current status of research and development in the field of nuclear-radiation spectrometry with detectors based on inorganic scintillators is surveyed. The results of investigation of the characteristics and applications of such scintillating monocrystals as cesium iodide, bismuthorthogermanate, and barium fluoride, which are widely used in experiments, are systematized. The progress in developing new types of scintillators is described. Special attention is paid to the precision calorimetry of high-energy electromagnetic radiation based on the use of inorganic scintillators.

1. INTRODUCTION

The early period of the development of scintillation detectors based on inorganic monocrystals is discussed most completely in the well known monograph of Birks.[1] These crystals have mainly been used for low-energy gamma spectrometry. The faster organic scintillation counters have dominated in high-energy physics.[2] In the early 1960s inorganic scintillators were also squeezed out of low-energy spectrometry by the more precise semiconductor detectors. Inorganic scintillators reappeared in the 1970s, when it became acutely necessary to have spectrometric detectors of large size and multichannel spectrometric setups with 4π geometry. Here at first NaI(Tl) monocrystals dominated.[3] However, in later years CsI(Tl) monocrystals came to be used more and more, especially in conjunction with solid-state photodetectors. The use of such monocrystals as bismuthorthogermanate (BGO) and barium fluoride (BaF_2) gave different results. At present, work continues on improving the characteristics of detectors based on these crystals and modifications of them. New promising scintillating materials have appeared.

The range of applicability of detectors based on inorganic scintillators is very broad, both in science and in applied research. The multitude of problems and special conditions in various physics experiments definitely affect the design of the detectors used. Standard detectors manufactured by industry can often be used for applied research (see, for example, Ref. 4).

In this review we attempt to systematize and generalize the publications on detectors based on inorganic scintillators and their use in modern experimental physics. Below, we give the notation and description of the scintillator characteristics most frequently encountered in the text.

- η is the conversion efficiency of luminescence or simply the scintillation efficiency. This is the fraction of energy which is realized as scintillations.
- The technical light output (or simply the light output or yield) is related to the number of photoelectrons produced in a photodevice under the action of a scintillation. The light yield is often expressed as a percentage of the light yield of NaI(Tl).
- τ is the scintillator luminescence time, defined in terms of the exponential $e^{-t/\tau}$.
- Λ_0 is the optical length of light attenuation. The light intensity decreases by a factor of e over this distance.
- $\lambda_{\max}$ is the wavelength corresponding to the maximum of the scintillator emission spectrum.
- d is the scintillator density.
- E_c is the electron critical energy at which the losses to bremsstrahlung and ionization are identical.
- X_0 is the radiation length characterizing the efficiency with which a given material absorbs electromagnetic radiation: photons, electrons, and positrons.
- The average energy of an electron beam at energies $E \gg E_c$ decreases by a factor of e upon passage of the beam through a layer of matter of thickness X_0. The interaction of electromagnetic radiation with matter produces a cascade (shower) of photons, electrons, and positrons, which develops until the electron and positron energy reaches E_c. The shower depth is measured in units of X_0.
- R_M is the Molière radius characterizing the shower size in the transverse direction,
- $R_M = X_0(Z+1.2)/37.34$ (Ref. 5). A cylinder of radius $3R_M$ contains 99% of the shower energy.
- Λ_I is the nuclear interaction length. It is the scale for the spatial development of the hadron shower arising as a result of the strong interaction of high-energy particles (energy greater than 10 GeV) with the scintillator material. It can be defined as the mean free path for protons between inelastic interactions.[6] For pions this path is about 1.5 times larger.
- The ratio X_0/Λ_I for an electromagnetic detector should be minimized in order to decrease the hadronic background.
- At low energies the efficiency with which γ quanta are recorded by the scintillator is often characterized by the coefficient describing the absorption of γ quanta of known energy by a layer of matter of a given thickness, for example, 1 cm.
- The energy resolution of a spectrometer at high energies is usually characterized by the rms deviation σ, while at low energies it is characterized by the full width at half-max (FWHM) and sometimes by the width at one tenth of the maximum (FWTM).

 1063-7796/94/010092-26$10.00

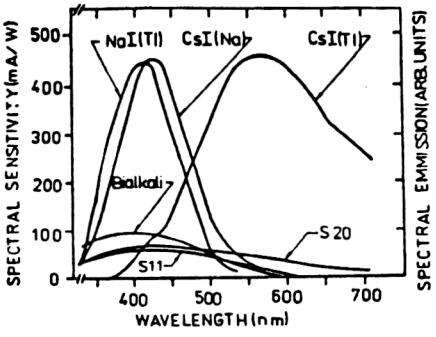

FIG. 1. Emission spectra of NaI(Tl), CsI(Tl), and CsI(Na) and spectral sensitivity of several types of photomultipliers.

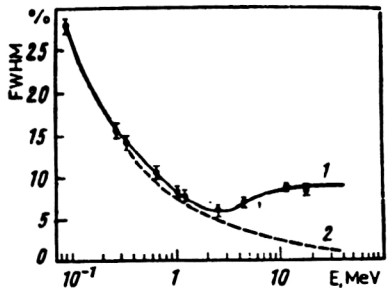

FIG. 2. Energy resolution of a detector using a NaI(Tl) crystal of diameter 125 mm and height 100 mm as a function of the γ energy.

2. SODIUM IODIDE

Monocrystalline sodium iodide doped with thallium NaI(Tl) is a classical scintillator for detecting γ radiation. Discovered by R. Hofstadter more than forty years ago, to this day it remains widely used. This scintillator is distinguished by its high light output: it takes about 25 eV to produce a single photon in it. Here the luminescence spectrum (see Fig. 1), which has a maximum at $\lambda \approx 415$ nm, closely matches the spectral sensitivity of standard photocathodes. The monocrystal is highly transmissive for the light of its intrinsic radiation ($\Lambda_0 = 2$ m) and relatively simple to prepare. Its scintillation efficiency is $\eta = 0.13$, and the luminescence time is $\tau = 230$ nsec. However, 0.5–5% of the light emission occurs in long-time components (more than 3–6 msec). A great defect of this crystal is its high hygroscopicity. Reliable shielding from moisture is necessary. Crystals are hermetically packed in containers. A roughened, diffusive reflector (usually MgO) is deposited on the side surface (usually cylindrical) and one of the ends. This significantly improves the light collection. The index of refraction of the crystal is $n = 1.85$. The light falls onto a photosensitive surface through glass having lower index of refraction ($n_0 = 1.49$) than the crystal. When the contact between the crystal and the glass is dry, there is a layer of air with index of refraction equal to unity. However, usually optical contact is created by means of an immersion layer of lubricant with index of refraction near n_0. Since $n/n_0 > 1$, the light is partially reflected from the glass. The diffusive reflector directs a significant fraction of this light back to the photocathode. In small crystals the light-collection coefficient can reach 70%. Here, if $E = 1$ MeV, the number of photons falling on the light-sensitive surface will be $N = \omega\eta E/E_{ph} = 3 \cdot 10^4$ ($E_{ph} = 3$ eV is the average photon energy).

For a small crystal the energy resolution is mainly determined by the photoelectron statistics. It is standard to measure the energy resolution for the 662-keV γ line from a ^{137}Cs radioactive source. The best resolution obtained for a crystal of diameter $D = 25$ mm and height $H = D$ was 5.6% (Ref. 7). The resolution is usually 6.5–7.5% for crystals of size up to $D = H = 8$ cm and 7.5–10% for larger sizes.

In particular, the behavior of the resolution for $D = 125$ mm and $H = 100$ mm has been studied as a function of the γ energy. As the energy is increased to 2.5 MeV the resolution improved along with the photoelectron statistics, nearly following the calculated dependence (Fig. 2). However, the resolution became worse at higher energies. The reason for this is fluctuations of the energy leakages arising from the fact that the crystal size was too small. Increasing the size to $D = 24$ cm and $H = 25$ cm made it possible to improve the energy resolution to 2.2% for $E = 22$ MeV (Ref. 8). Here to eliminate events with energy leakage, the crystal was surrounded by an anticoincidence counter. A giant monocrystal with $D = 77$ cm and $H = 51$ cm scanned by 12 photomultipliers ($D = 8$ cm) in a beam of electrons with $E = 15$ GeV displayed a resolution FWHM = 1.2% (Ref. 3). These sizes corresponded to $D = 18R_M$ and $H = 19.7X_0$. We note that extension of the detector length to $\sim 20X_0$ or more is usually a standard requirement in constructing an electromagnetic calorimeter. The transverse dimension is related more to the geometry of the experiment.

For high efficiency of recording γ quanta in the case of multiple production it becomes necessary to use a multidetector setup. 4π geometry has been obtained by using NaI(Tl) crystals in the spin spectrometer (Ref. 9) and the Crystal Ball detector (Ref. 10).

Under room conditions the light yield of NaI(Tl) is a maximum; the temperature coefficient is 0.22–0.5%/°C and depends on the sample. Below 0 °C and above 60 °C the light yield falls considerably. A decrease of the temperature is accompanied by a worsening of the intrinsic resolution of the monocrystal as a result of the appearance of inhomogeneities in the light yield. It has been noted[4] that this is to a large degree manifested with increasing concentration of the dopant, i.e., at low temperatures a lower thallium concentration is preferable. The luminescence time of the scintillator also depends on the temperature. It decreases with increasing temperature, first steeply down to 150 nsec near 60 °C, and then more smoothly down to 100 nsec (Ref. 4).

The luminescence time also depends on the ionization density, which has been used to separate protons, α particles, and γ quanta at energies below 10 MeV (Refs. 11 and 12).

At room temperature a NaI monocrystal which is not doped with thallium has too low a light yield. However, if it is cooled to liquid-nitrogen temperatures, it displays a strong growth in the light yield, which is almost twice that of the light yield of NaI(Tl) at 20 °C (Ref. 13). Luminescence occurs with a time constant of 60 nsec at a wavelength of $\lambda_{max}=303$ nm.

3. CESIUM IODIDE

Monocrystals doped with thallium and sodium

The need for hermetic packing of NaI(Tl) crystals leads to a corresponding constraint on their simultaneous use as gamma-ray detectors and as detectors of low-energy charged particles. In this respect CsI(Tl) is preferable, because it is not hygroscopic. However, for long-term use the monocrystal must be isolated in a dry ambient medium, and small flows do not lead to its breakdown, as in the case of NaI(Tl). The plastic nature of cesium iodide makes it easy to work mechanically, in contrast to sodium iodide, which tends to decompose or crack under mechanical or thermal stresses. The use of cesium iodide makes it possible to construct detectors in a wide variety of shapes and sizes.

The radiation length of CsI(Tl) is $X_0=1.85$ cm, i.e., smaller than that of NaI(Tl). The index of refraction is $n=1.80$.

The emission spectrum of CsI(Tl) has a maximum at $\lambda=550$ nm (Fig. 1) and is not well matched to the characteristic of the standard S-11 photocathode. With this photocathode the amplitude of the signal from CsI(Tl) is usually 45% of the amplitude of the signal obtained from NaI(Tl). A photocathode of the S-20 type is more suitable for CsI(Tl). For higher sensitivity of the photocathode in the green region and signal-formation time constant of order 5 μsec its amplitude is increased to 85% (Ref. 14). The need for such a long signal is dictated by the large luminescence time of the crystal (~ 1 μsec), which, of course, is a drawback of this scintillator. The scintillation efficiency of CsI(Tl) is even somewhat higher than that of NaI(Tl). According to Ref. 15, for energy losses of 1 MeV in NaI(Tl), 40×10^3 photons are produced, while for CsI(Tl) the number is 45×10^3.

The crystal doped with sodium rather than thallium is better matched to the S-11 spectral characteristic (see Fig. 1). Here also the luminescence time is decreased to 630 nsec. The amplitude of a pulse from CsI(Na) is 85% of that of a pulse from NaI(Tl) (Ref. 13). Moreover, according to Ref. 16, the former is just as good as the latter in its scintillation efficiency, but CsI(Na) is much less hygroscopic than NaI(Tl). A deficiency of CsI(Na) and CsI(Tl), as for NaI(Tl), is the rather large afterglow: up to 5% in 3–6 msec, which significantly restricts the counting rate.

The technology for preparing cesium iodide, especially CsI(Tl), is not very complex. CsI(Tl) is relatively cheap, even in the large sizes needed in the construction of electromagnetic calorimeters.[17]

Recently, there is wider and wider use of silicon photodiodes as photodetectors, as they are small and insensitive to the magnetic field of scintillation detectors.[18] A CsI(Tl) crystal with the correct spectral characteristic is particularly well matched to such a photodetector (Fig. 3).[19] At the emission peak of the crystal the quantum photodiode yield is about 65%. Using photodiode information readout, 32×10^3 photoelectrons per MeV have been obtained.[15] Replacement of a photomultiplier by a photodiode significantly decreases the temperature dependence of the detector (Fig. 4).[15] The photoelectron yield acquires a flat maximum at 30–40 °C and coefficient 0.3%/ °C at 20 °C. Measurements have been carried out using S-1790 photodiodes from the Hamamatsu company. These diodes and four CsI(Tl) crystals were used to construct a test calorimeter in a beam of electrons of energy 1–20 GeV (Ref. 20). An individual crystal was 10 cm long and 10.5 cm in diameter. The light yields of the four crystals measured at the photodiodes varied within a 10% range. Two crystals were joined end to end by an optical lubricant to form a section. Eight photodiodes were attached by optical lubricant to one face and connected in parallel. The crystals were wrapped in several layers of white teflon tape, and then in aluminum foil and black paper. The two sections were placed right next to each other with the photodiodes at opposite ends. The signals from the photodiodes were amplified by two amplifiers with a shaping time of 3 μsec. For α particles of energy 5.5 MeV the signal amplitude was 70% compared with the signal from particles with minimum ionization at the same energy release. The density of the ionization from these particles and the α particles differed by more than a factor of 150. This feature, the high ratio α/β, should ensure the required linearity of the light yield at the maximum energies, when a large number of slow particles is formed at the end of a shower. The measurements displayed linearity of the light yield in the entire range quoted above.

The resolution of this calorimeter, whose length was

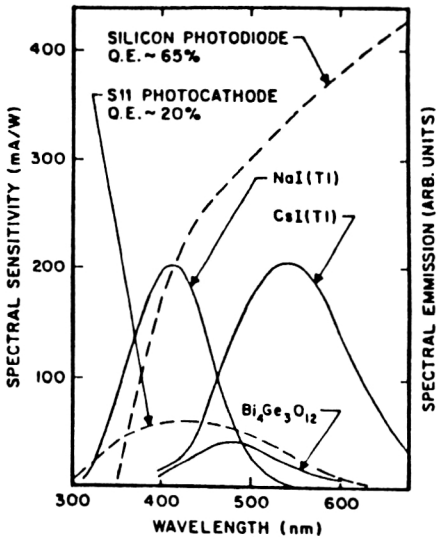

FIG. 3. Emission spectra of CsI(Tl), NaI(Tl), and BGO, and spectral sensitivities of silicon PIN photodiodes and a photomultiplier with an S-11 photocathode.[19]

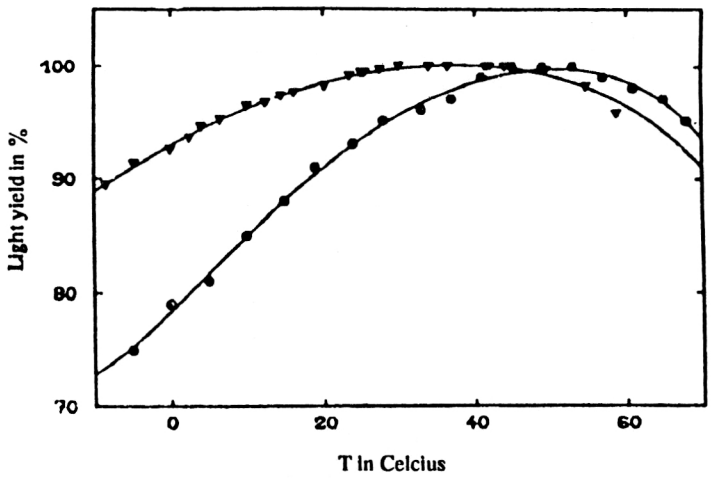

FIG. 4. Temperature dependence of the relative light output measured by a photodiode (Hamamatsu S-1790, △) and a photomultiplier (S-11, ●). Both curves are normalized to 100% (Ref. 15).

$22X_0$, was $\sigma=1.6\%$ at the end of the energy range. It also includes the beam spread, which is 1%. Good separation of electrons (e) and hadrons (h) was obtained. The ratio e/h in the range $\pm 2\sigma$ about the electron peak was 1.14×10^3 at 4 GeV and 3.8×10^3 at 10 GeV.

Eight thousand crystals 30 cm long and 5×5 cm in cross section with four photodiodes on each were used to construct the CLEO-2 calorimeter installed at the Cornell electron storage ring.[19] The results from a test calorimeter made of nine such modules, the central one of which was bombarded by a positron beam, are presented in the same study. An amplitude analysis of the total signal was performed. The noise of the photodiodes and preamplifiers was FWHM = 3 MeV, and its effect was significant only for $E<100$ MeV. In the range 0.1–2 GeV the main contribution to the resolution came from transverse leakages, and at higher energies it came from leakage from the rear face. The contribution of noise, transverse, and longitudinal leakage at $E=0.1$–5 GeV is illustrated in Fig. 5. We see that at the end of the range the resolution is $\sigma/E=1.5\%$.

In a different electromagnetic calorimeter, designed for experiments at the low-energy antiproton ring (LEAR) at CERN, the number of photodiodes is greatly decreased, owing to the use of spectrum-shifting light guides.[21] The light guide is a Plexiglass plate 3 mm thick bordering (but without optical contact) the light-collecting face of a CsI(Tl) crystal (similar to that shown in Fig. 18 for a different type of scintillator). Material which actively absorbs light arriving from the scintillator and reemits it at longer wavelengths is introduced into the Plexiglass (see Fig. 6). The reemitted light is distributed isotropically. Owing to total internal reflection on the walls of the plate, a significant fraction of it falls on the photodiode attached to the narrow face of the plate. In this way light is concentrated on a light-sensitive surface which is many times smaller than the area of the light-collecting face. Crystals in the form of truncated pyramids of length 30 cm were used. The calorimeter is composed of 1380 such modules forming a kind of "barrel" with solid angle close to 4π.

CsI(Tl) crystals combined with photodiodes are also used in astrophysics. They have been used to construct a calorimeter to measure the energy and direction of high-energy (0.1–100 GeV) cosmic γ rays.[22]

It has been shown that cesium iodide is distinguished by an extremely low level of intrinsic radioactivity. In addition, the compactness of a detector using a photodiode makes it easy to shield it from the surrounding medium. These features have been used in designing a device for seeking 2β decay from ^{100}Mo (Ref. 23). Molybdenum film was placed between crystals of diameter 7.5 cm and thickness 5 cm, to each of which were attached five S3204-03 photodiodes. This photodiode is made of high-resistance silicon, which made it possible to increase the thickness of its p–n junction, and as a result lower the capacitance to 43 pF/cm, instead of the 100 pF/cm of the types mentioned earlier. The area of the new photodiode is 1.8×1.8 cm, and the leakage current is 6 nA. The photodiode capacitance

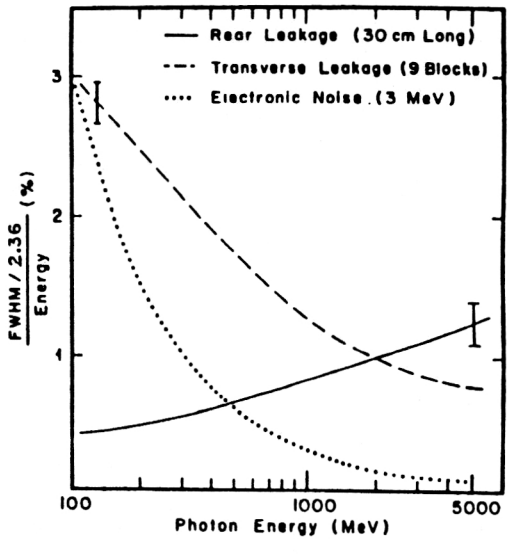

FIG. 5. Contribution to the energy resolution in blocks of CsI(Tl) due to the three dominant sources: rear leakage from the 30 cm-long crystals, transverse leakage from the nine square crystals 5 cm on a side, and electronics noise, assumed to be 3 MeV (Ref. 19).

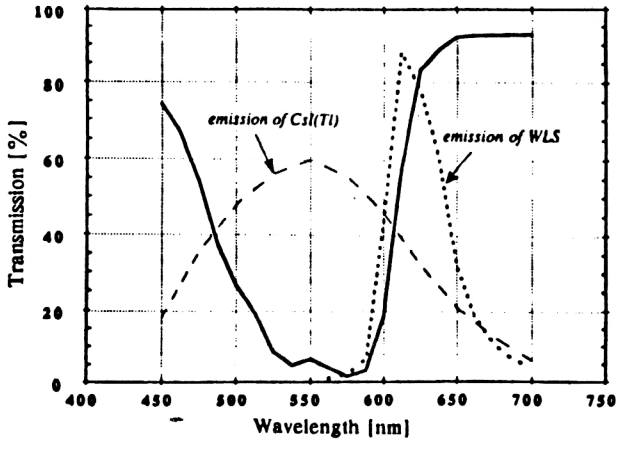

FIG. 6. Optical matching of a CsI(Tl) scintillator with a wavelength shifter. The dashed line is the spectral emission of CsI(Tl) (schematic). The solid line is the measured transmission of the wavelength shifter. The dotted line is the measured spectral emission of the wavelength shifter.[21]

and leakage current determine the noise, which in this detector was 150 keV (FWHM). This resolution is quite acceptable for an experiment. In the case of 2β decay two electrons with a total energy of 3 MeV would be produced. As a result of passage through the molybdenum layer, this line is smeared to a width close to 150 keV. It is important that the crystal, which is not hygroscopic, practically has no dead layer for electrons. Another property of the detector which is very important for extended measurements is the weak dependence of the signal amplitude on the temperature and stability of the time readings.

Features of a scintillation of CsI(Tl) and their use

The light emission of CsI(Tl) has a finite rise rate which depends both on the thallium concentration and on the ionization density. This is illustrated in Fig. 7, in which we give the data for β and α particles as a function of the concentration by weight of C (Ref. 24).

The ionization density also affects the luminescence time of CsI(Tl). A scintillation pulse can be fitted by two exponentials, one with a relatively small time constant $\tau_f=0.4$–0.7 μsec, and the other with a long one $\tau_s=7$ μsec

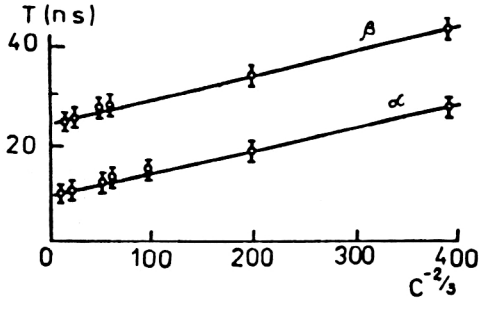

FIG. 7. Rise time of a scintillation in CsI(Tl) as a function of the Tl concentration for β and α particles.[24]

(Refs. 25–28). In Refs. 29 and 30 the value $\tau_s=4$ μsec is quoted. This component is independent of the type of particle, while the fast part of the pulse does depend on the type.

In Ref. 29 for α particles of energy 95 MeV the pulse was fitted well with $\tau_f=0.8$ μsec. For α particles of energy 5 MeV two components with $\tau_1=0.7$ μsec and $\tau_2=0.24$ μsec were introduced.[15] Their intensity ratio was $I_2/I_1=0.77$. The pulses for α particles, which have large ionization density, are considerably shorter than for weakly ionizing γ rays, for which the luminescence time was 0.9 μsec.

Therefore, both the pulse rise time and the pulse duration and height in a CsI(Tl)-based detector depend on the type of recorded particle. This makes it possible to separate particles by pulse-shape discrimination (Refs. 31–33 and 27). In particular, this possibility was foreseen in PEGAS, a multimodule spectrometer with 4π geometry for γ quanta and charged particles.[34]

Rather good resolution of p, d, t, and α according to the pulse duration was observed for $E=40$–70 MeV at a counting rate of $N=10^3$ sec^{-1} (Ref. 27). However, for $N=1.4\times10^4$ sec^{-1} the resolution was no longer satisfactory. For these particles, and also for α and He^3 at this counting rate the separation was accomplished by using the $(\Delta E$–$E)$ technique. Here ΔE was measured by a silicon detector of thickness 400 μm, and most of the particle energy was measured by a CsI(Tl) crystal with a photodiode.

It should be noted that the best energy resolution was obtained in a $(\Delta E$–$E)$ system completely made up of semiconductor detectors. However, the insufficient thickness of such detectors imposes a corresponding constraint on the particle energy. Stacks of these detectors can be used, but for large (4π) multidetector systems this is expensive. In addition, thick semiconductors are sensitive to radiation damage.

For these reasons, whenever the energy resolution is not the most important factor, CsI(Tl) is successfully used as the residual-energy detectors. This is particularly true of experiments involving heavy ions at intermediate energies (10–100 MeV/nucleon). It is important that CsI(Tl) is not hygroscopic, so that the "dead" layer between it and the ΔE detector can be small.

Sufficiently high resolution is obtained for charged particles by using CsI(Tl). For example, Ref. 27 quotes the value FWHM=1% for protons of energy 54.7 MeV. The dependence of the light yield on the proton energy is found to be practically linear, as shown in Fig. 8 (Ref. 35) along with data for other light particles up to $Z=8$. The light yield for particles up to $Z=40$ is given in Ref. 36. A combination of a thin silicon ΔE detector and a thick $(E$–$\Delta E)$ detector based on CsI(Tl) made it possible to reliably separate particles in charge and mass (Refs. 27, 30, and 35–37).

We note that in the last of the cited studies a significant dependence on the mass number A was observed in addition to the expected dependence of the light yield on Z and E. A simple parametrization was given which allows the

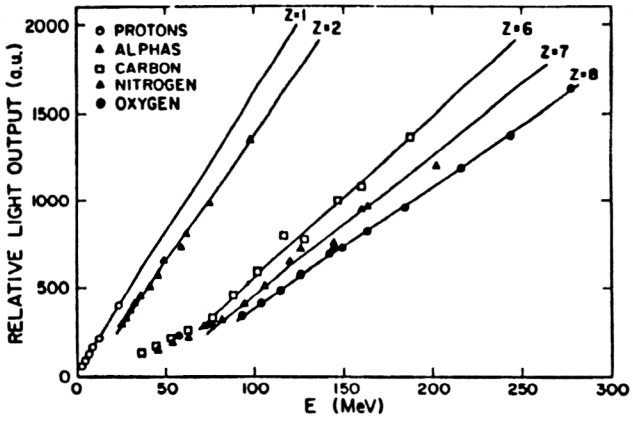

FIG. 8. Light output of CsI(Tl) as a function of energy for C, N, and O ions, compared with the crystal characteristic for protons and α particles.[35]

light yield L for different Z, E, and A to be determined by using the well known Birks formula:[1]

$$dL/dX=(dE/dx)/(1+[kB(dE/dX)]),$$

where kB is the Birks constant.

For energies above several MeV a good approximation is $dE/dx=cAZ^2/E$. Integration and use of the experimental data lead to the following expression for the light output:

$$L=a_0+a_1\{E-a_2AZ^2\ln[(E+a_2AZ^2)/a_2AZ^2]\},$$

where $a_0=28.0$, with the standard error corresponding to 0.7 MeV, $a_1=8.145\pm0.036$, and $a_2=0.321\pm0.003$.

Fast monocrystals

The introduction of thallium into crystals of cesium iodide raises the light output by an order of magnitude, but at the same time makes the crystal slow. Pure CsI luminesces after several nonoseconds in the ultraviolet region for $\lambda_{max}=310$–320 nm (Refs. 24–46 and 38–40). Slow components of duration 0.1 μsec and 1 μsec with luminescence spectrum at $\lambda=360$–600 nm are also observed (Fig. 9).[39] It is thought that these components arise from spoiling of the crystal lattice structure and can be practically absent in crystals of high quality. The dependence of the crystal characteristics on how the crystal is prepared is discussed in Ref. 40. Crystals grown in the standard manner have components with $\tau=3$ μsec with intensity 26% of η_0 for electrons, where η_0 pertains to NaI(Tl). This component is practically not observed in crystals prepared by zonal melting, and is completely absent when the cold-pressing technique is used. In the first case the luminescence by intensity (relative to η_0) is 1.2% with $\tau_1=1.8$ nsec and 3.8% with $\tau_2=12.9$ nsec, and in the second case the numbers are 1.6% with $\tau_1=1.0$ nsec and 2.4% with $\tau_2=9.6$ nsec.

Pure CsI is slightly hygroscopic. Crystals can be prepared in the same sizes as ones doped with thallium.

Crystals of the type CsI–CsBr, which have a light yield of $0.18\eta_0$ and luminescence time of 11 nsec in the range 280–340 nm, are interesting.[41] Results have been obtained for a crystal of cross-sectional area 2.5×2.2 cm.

4. BISMUTHORTHOGERMANATE

Basic characteristics

The chemical formula of this scintillator,[42,43] usually called BGO, is $Bi_4Ge_3O_{12}$. The centers of luminescence in the monocrystal are the bismuth ions, and they do not need dopants. The main advantage of BGO is its small radiation length $X_0=1.13$ cm. A given volume of BGO crystal allows a much larger γ detection efficiency than the same volume of the crystals discussed above.

The luminescence spectrum of the crystal is shown in Fig. 3. It lies somewhat farther to the right ($\lambda_{max}=480$ nm) than the sensitivity spectrum of the S-11 photocathode. The index of refraction of the crystal $n=2.13$ is considerably larger than that of the glass of the photomultiplier. Both of these factors tend to lower the number of photoelectrons.

A technical difficulty is the formation of air bubbles inside the crystal volume when it is prepared. Scattering with consequent light loss occurs on these bubbles. Compared with NaI(Tl), the number of photoelectrons from BGO can range from 8% to 16%, depending on the quality

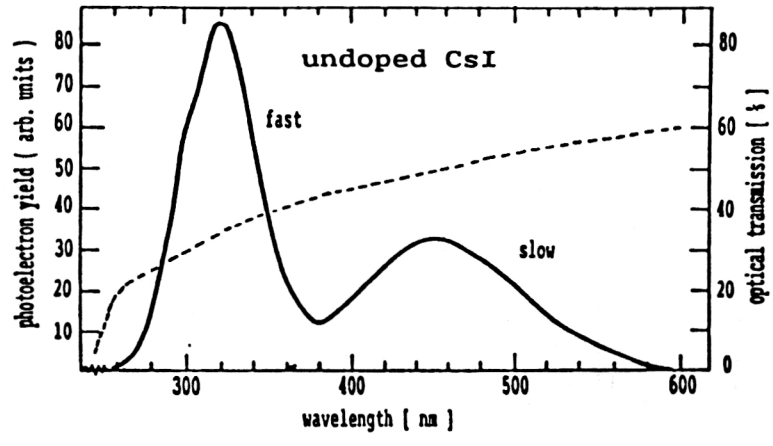

FIG. 9. Emission spectrum of an undoped CsI crystal of length 25 cm irradiated by 30-keV x rays and optical transmission of the crystal.[39]

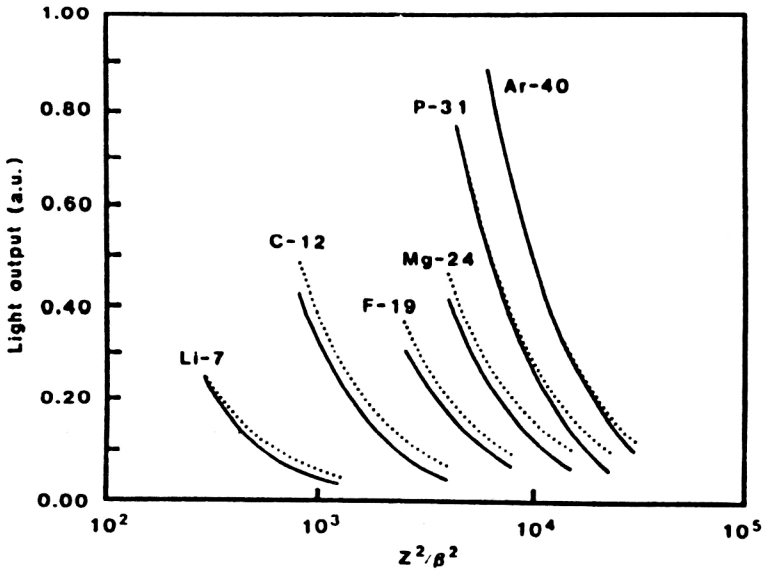

FIG. 10. Normalized relative light output of BGO and CsI(Tl) for several ions. The solid lines are the light output for BGO, and the dashed ones are for CsI(Tl) (Ref. 36).

of the crystal and its dimensions. A value of even 20% has been quoted.[44]

The luminescence time of BGO at room temperature is 30 nsec, i.e., slightly worse than that of NaI(Tl). However, in contrast to the latter, the afterglow in the millisecond region is very small for BGO: 0.005%. Therefore, on the whole BGO is faster than NaI(Tl). The duration of a scintillation of BGO depends strongly on the temperature. At 0 °C it is 400 nsec, and at 40 °C it is $\tau=200$ nsec. The light output also depends strongly on the temperature. The temperature coefficient is 1.55%/ °C under room conditions.[45]

The considerably smaller resulting light yield of BGO in comparison with NaI(Tl) is accompanied by a corresponding worsening of the energy resolution. Among the better results are a resolution of 9.3% for γ radiation from ^{137}C for a crystal (Harshaw brand) of cross section 25×25 mm, obtained from doubly recrystallized raw material.[46] Since the transmission of their intrinsic radiation is poor for BGO crystals, their resolution is observed to depend significantly on their size. For example, whereas for a crystal of cross section 25×25 mm the resolution is 10.5%, for one of cross section 25×100 mm prepared from the same raw material it is 13.3% (Ref. 47).

Advantages of BGO are its good mechanical properties under processing and its nonhygroscopicity. Owing to its high γ detection efficiency, BGO can be used to make compact devices widely used in tomography and as an active shield from background.

Like CsI(Tl), BGO in conjunction with a thin silicon detector can be used to separate particles in charge and mass in a wide range of energies.[36] Here the dependences of the light yield on the type of particle and on the particle speed β for the two crystals are close to each other (Fig. 10).

The high density of BGO allows the creation of compact spectrometric detectors for the absorption of both electromagnetic radiation and charged particles (see, for example, the BGO ball in Ref. 48). In particular, protons of energy up to 450 MeV are absorbed over a length of 24 cm. Crystals of this length with a trapezoidal form have

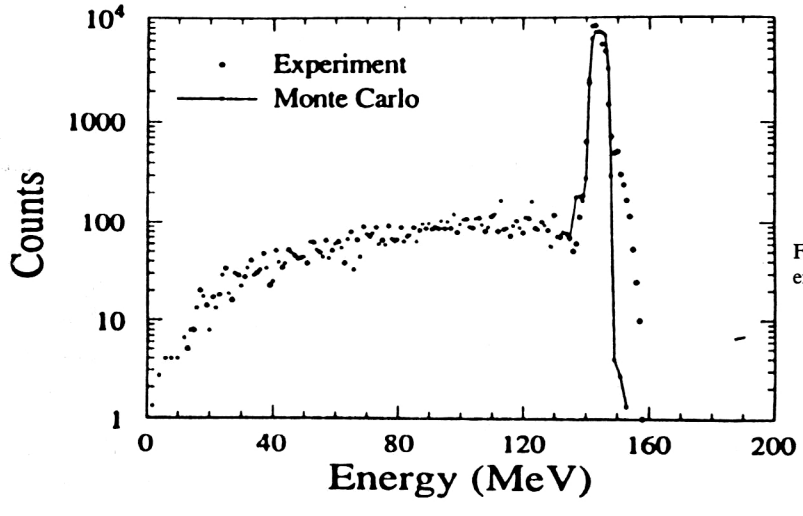

FIG. 11. Experimental and Monte Carlo spectra for protons of energy 144.5 MeV (Ref. 49).

TABLE I. Ratio of the low-energy tail and the main part of the proton spectrum near the peak at various energies.

E, MeV	30	50	70	90	100	110	130	150	160	170
Fraction, %	1	3	5	8	10	12	16	20	22	27

been used to make a 4π calorimeter designed to study photonuclear reactions for photon energies up to 2 GeV (Ref. 49).

However, the spectrum from protons and other charged particles turns out not to be as narrow as that from electromagnetic radiation. It is extended in the direction of smaller losses, owing to nuclear interactions. A typical spectrum is shown in Fig. 11. The contribution of the low-energy tail grows with increasing proton energy, as illustrated in Table I.

Spectrometry of hard electromagnetic radiation

At energies $E \gtrsim 20$ MeV the photoelectron statistics already become unimportant for the resolution. It is important that the volume of the BGO crystal can be chosen to be an order of magnitude smaller than for a NaI(Tl) crystal, which accordingly lowers the sensitivity to the surrounding background of γ quanta and neutrons. This means that the former crystal is better than the latter in the spectrometry of γ quanta of relatively high energies when there is a large background from low-energy γ quanta and neutrons. Relative measurements have been made for crystals of both types with cross section 38×38 mm (Ref. 50). At the energies 666, 1332, and 2754 keV the count from BGO is higher by factors of 3.3, 4.5, and 5.6, respectively. The efficiency of NaI(Tl) falls off more sharply with increasing energy than does that of BGO. Even for the same volume BGO is less sensitive to neutrons than is NaI(Tl) (Ref. 51). Relative to the sensitivity of NaI(Tl) to neutrons with energies $E \geqslant 5.0$, 3.5, and 0.5 MeV, the sensitivity of BGO was 1.2, 1.0, and 0.2 (Refs. 42 and 52). A sensitivity of less than 0.1 is predicted for $E_n < 0.5$ MeV.

In certain experiments a lower detector sensitivity to a low-energy background of γ quanta and neutrons can be more important than a higher energy resolution. This is why, for example, in Ref. 53 BGO was preferred over NaI(Tl). For crystals of cross sections 2.54×2.54 cm and 7.62×7.62 cm the resolution FWHM at 6.14 MeV was 4.5% and 5.6%, respectively.

A BGO spectrometer for 10–100 MeV photons with low sensitivity to room (γ and n) background is described in Ref. 54.

For $E = 10$–300 MeV at the TRIUMF accelerator a spectrometer was designed on the basis of BGO crystals of length 21 cm in the form of rectangular bars of thickness 4 cm and truncated pyramids with faces of area 2×2 cm and 3×3 cm (Ref. 55). An XP-2230 photomultiplier is attached to the latter. The two faces and two opposite sides are polished, and a reflector is laid on the other two, which are unpolished. A popular reflector like MgO did not give the best results. The best were obtained using a three-layer combination: yellow tape, white paper, and black tape. Here the nonuniformity of the module along its length, except for 2 cm near the face, was 1%, and the resolution from γ rays of energy 662 keV was $\Delta E/E = 15\%$.

A negative factor for light collection at the photocathode is the fact that the index of refraction of the BGO crystal is significantly larger than that of glass. However, if the crystal is cone-shaped, its longitudinal nonuniformity is decreased enough that the contribution of the latter (σ_{dis}) to the total energy resolution (σ_{tot}) becomes small. For example, $\sigma_{\text{dis}} = 0.2\%$ was obtained for $\sigma_{\text{tot}} = 0.94\%$ for $E = 1$ GeV in the 4π spectrometer designed for studying photonuclear reactions up to ~ 2 GeV at Frascati.[56] The nearly 4π geometry of the spectrometer is produced by 480 sections with eight different pyramidal shapes.

A calorimeter of 12 crystals of dimensions $3 \times 3 \times 20$ cm with photodiode information readout has been tested in a beam of electrons and pions with energy up to 10 GeV (Ref. 57). The energy resolution for $E > 1$ GeV was $\sigma/E = 1\%$; it was determined mainly by fluctuations of the shower leakages and also by the photodiode noise. The electron–hadron separation inside an energy window of $\pm 2\sigma$ about the electron peak was better than 1:500 in the entire energy range 0.5–10 GeV. It could be improved by a factor of two by simply truncating the data.

The high density and very short radiation length of BGO, together with the near absence of dead layers between crystals, made it possible to design a very compact electromagnetic spectrometer for experiments at the Cornell electron storage ring.[58] The calorimeter was inserted inside an array of NaI(Tl) crystals constructed earlier, which performed the function of a leakage detector. The energy resolution was 1% at 5 GeV and 2% at 100 MeV.

A BGO spectrometer surrounded by NaI(Tl)-based counters is also described in Ref. 59. The spectrometer is designed to measure photon energies in the range 200–1500 MeV at the Frascati accelerator for a counting rate of up to 10^4 per second. NaI(Tl) crystals connected in anticoincidence form a background shield.

A detector on a large scale is the electromagnetic calorimeter of the L3 setup at the LEP accelerator at CERN, composed of 11 488 BGO crystals (Refs. 60 and 45). An individual crystal has a length of 24 cm ($21.4X_0$) and the shape of a truncated pyramid with faces of area 2×2 cm and 3×3 cm. The crystal is covered with NE560-type paint. Light is collected by two silicone diodes. The crystals are arranged along radii running from the point where the colliding beams intersect. They form a "barrel" encompassing a nearly 4π solid angle. The energy resolution for electrons at $E = 100$ MeV was $\sigma = 5\%$ and better than 1% for $E > 2$ GeV.

Spectrometry using such a large number of channels requires the continuous calibration of these channels. A

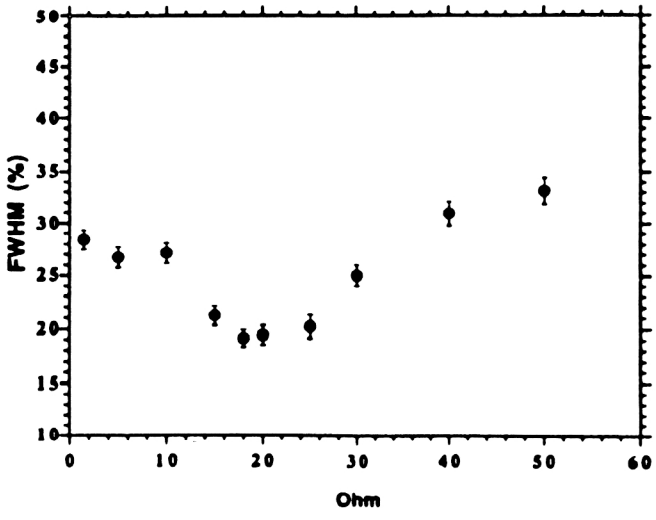

FIG. 12. Energy resolution of a detector with a BGO crystal for γ rays from ^{137}Cs as a function of the value of the trimmer attached to the end of the coaxial cable; the anode pulse is cut off at 100 nsec (Ref. 62).

small radio-frequency quadrupole accelerator which emits γ quanta of energy 1.85 MeV was developed for this.[61]

A BGO crystal, like a NaI(Tl) crystal, has a rather long luminescence time, which leads to a corresponding limitation in experiments with a high counting rate. The coincidence problem which arises here can be overcome to some degree by clipping the pulse from the photomultiplier. It has been shown[62] that pulses from a BGO detector can be clipped very cleanly by using the signal-reflection technique, without significantly worsening the energy resolution. Studies have been carried out with a crystal of length 24 cm having the shape of a truncated pyramid. A photomultiplier (R-329, Hamamatsu) was optically connected to the face of cross section 6.5×5.5 cm. The opposite face had cross section 1.2×1.9 cm. The signal shaping was performed by connecting a segment of 50-Ω cable to the photomultiplier anode. A compatible resistance of 50 Ω was always connected on the anode side, and a variable resistor (trimmer) was connected to the opposite end. The energy resolution from ^{137}Cs without pulse clipping was 15.7%. The clipping of the photomultiplier pulses for $\Delta t = 100$ nsec led to a 15–20% decrease of the amplitude and a resolution of 19.3% for a trimmer of 15–30 Ω. This turned out to be the optimal choice (Fig. 12). The resolution worsened with decreasing Δt, and almost did not change with increasing Δt. The explanation of this behavior is related to the effect of electronics noise. This effect should decrease with increasing signal amplitude. In fact, for $E_\gamma = 15.1$ MeV a resolution of 8% was obtained, both with the pulse clipped to 200 nsec and without clipping. These measurements were carried out with the BGO spectrometer described in Ref. 54. It is interesting to note that the same measurements with an equivalent NaI(Tl) crystal led to worsening of the resolution by 3–6% with pulse clipping. The authors relate the better behavior of BGO to the pure exponential falloff of its light pulse.

5. BARIUM FLUORIDE

Basic characteristics

Many physics experiments require the simultaneous measurement of both the γ (or electron) energy and the time at which the particle arrives at the detector. Plastic scintillators are usually used for precision time measurements, as they have a short luminescence time. However, their radiation length ($\sim$42 cm) is large, and the use of lead in a detector, in layers sandwiched between scintillator layers as a converter, makes it impossible to obtain good energy resolution. The discovery in the BaF_2 crystal, which has $X_0 = 2.05$ cm, of a fast component (0.6 and 0.76 nsec) raised scintillation γ spectrometry to a new level.[64] The luminescence spectrum of BaF_2 (Ref. 65) is shown in Fig. 15 (Ref. 66). Most of the light belongs to the component with $\lambda_{max} = 320$ nm, which has $\tau = 620$ nsec. Fast luminescence occurs in the region of wavelengths $\sim$200 nm. A photomultiplier with quartz glass is required to record ultraviolet light. The indices of refraction of BaF_2 and the glass must be close. According to Ref. 63, at 320 nm, BaF_2 has $n = 1.495$; for $\lambda = 200$ nm, $n = 1.63$, and for quartz $n = 1.53$ (Ref. 67).

The data on the light output of the crystal given in Refs. 14, 68, 69, and 127 are very contradictory. They give 8–20% of the light output of NaI(Tl). Not only the quality of the crystal, but also the technical difficulties arising in estimating the light output for various spectral ranges of the luminescence can affect the measurement results. The light output of BaF_2 relative to NaI(Tl) can be taken to be 5% for the fast component and 16% for the slow one. The crystal is weakly hygroscopic. Recent working of its surface increased the light output by 30% (Ref. 70). Hermetization of the crystal is needed to stabilize the light output. In the pioneering study of Ref. 64 the walls of the crystal were polished and covered (except for the light-collecting face) with Al_2O_3 white powder. MgO was also used as a covering, but the most popular is a several-layer-thick winding of teflon tape (up to $\sim$0.3 mm; Ref. 71). The teflon ensures a reflection coefficient of $r = 0.95$ in the ultraviolet.[67]

The optical contact between the crystal and the photocathode must be made with oil or lubricant with suitable index of refraction and transmission coefficient. In Table II (Ref. 72) we list the results of studies of several optical media.

As was shown in Ref. 73, in a thin layer of silicone lubricant such as Rhodorsil R-47, 100000*c SI* the light absorption at $\lambda = 220$ nm is less than 1%. According to the data of Refs. 71 and 74, water-free glycerin can successfully be used for optical coupling.

The main advantage of BaF_2 is the fact that the same time resolution can be obtained by using this relatively heavy crystal as can be obtained by using a plastic scintillator. For example, for a small crystal of cross section 2×1 cm a resolution of FWHM = 80 psec was obtained for γ

TABLE II. Measured number of photoelectrons when various oils and lubricants are used for BaF_2.

Oil/lubricant	Fast component, photoelectrons/MeV	Total light, photoelectrons/MeV	Fast component/ total light
DS 200	260	1580	16,5
Rhodorsil SI 300	235	1470	16,0
Rhodorsil 47 V	260	1575	16,5
Viscasil	260	1580	16,5
RTV 615 A+B	210	1495	14,0
V 788	123	1210	10,2
V 789	123	1200	10,3

rays of a radioactive ^{60}Co source (Ref. 64). Here for coincidence selection a second counter was used with an NE-111 plastic scintillator. The resolution due to fluctuations in the two counters was 112 psec. This quantity is $\sqrt{2}$ times greater than that given above for BaF_2, i.e., the contributions to the resolution from the first and second counters were the same.

For a crystal of cross section 9×9 cm and a plastic scintillator a time resolution of 375 psec (FWHM) was obtained for a ^{60}Co source at a threshold of 300 keV (Ref. 75).

For two large crystals of cross section 10×12 cm and 13.6×7.5 cm the resolution for a ^{60}Co source at a threshold of 300 keV was 590 psec (Ref. 73). The main reason for the worsening of the resolution with increasing crystal size is the time spread in the light travel from its point of origin to the photocathode. An additional worsening can arise from light loss in the bulk and at the walls of the crystal, and this increases with decreasing wavelength. At a distance of 12 cm from the scintillation point to the lower face of the crystal the light absorption was 9% for $\lambda=250$–290 nm and 12% for $\lambda=220$ nm.

The energy resolution for $E_\gamma=662$ keV of small (up to 4 cm) crystals connected to XP-2020 is 7–8% (Ref. 71), and for large crystals it is 10–12% (Ref. 76). As E_γ increases the energy resolution of BaF_2 becomes comparable to that of NaI(Tl), but BaF_2 gives a better time resolution. This is demonstrated by Table III (Ref. 77), in which we give the data for 4π spectrometers based on NaI(Tl) and BaF_2 crystals. Crystals of volume ~1 l have the rather complicated shapes of pentagonal and hexagonal prisms, which ensures a good detector geometry.

We note that the data on the energy resolution for $E=4.4$ MeV cannot be directly related to the type of detector material. Among the best values for $E_\gamma=662$ keV is the resolution of 9.3% obtained for a BaF_2 crystal of cross section 10×12 cm (Ref. 78). The resolution of this crystal was improved to 7.9% by cooling it to 243 K. The reason is that the light yield due to the slow component is increased sharply as the temperature is lowered. The temperature coefficient is 2.4%/°C (Ref. 79), which makes temperature stabilization necessary. It is remarkable that the fast component is practically independent of temperature.[80] By heating the crystal the slow component can be greatly weakened. This is used to increase the detector speed of response.[81–84]

Only the fast component of the light emission of BaF_2 can be used if a proportional counter with gas sensitive to the ultraviolet is used instead of a photomultiplier.[85]

Another method of raising the speed of response is that of doping the crystal with cerium[48,86] or lanthanum.[65,87] The optimal molar concentration of Ce is 4.4%. The introduction of Ce decreases the light yield by half, raises the luminescence time to 50 nsec, and shifts the luminescence spectrum to the right, to the region with a maximum at $\lambda=360$ nm. The light yield of BaF_2(Ce) and its luminescence time are practically independent of the temperature

TABLE III. Characteristics of 4π spectrometers.

Name		Spin spectrometer (Ref. 9)	Crystal-ball [10]	4π Spectrometer, Karlsruhe (Ref. 77)
Material		NaI(Tl)	NaI(Tl)	BaF_2
Energy resolution, %	662 keV	8,5	7,8	9,6
	1,3 MeV	6,3	5,5	7,1
	4,4 MeV		4,4	4,0
	6,1 MeV		4,0	3,6
Time resolution, nsec	FWHM	2,2	2,8	0,4
	FWTM	4,7	5,7	0,8

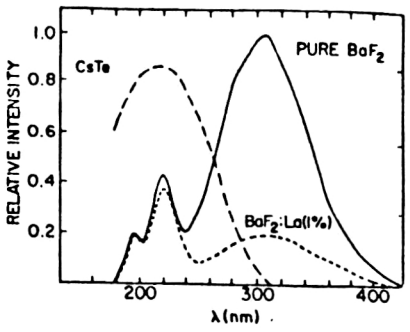

FIG. 13. Emission spectra of pure and lanthanum-doped BaF_2; quantum efficiency for the CsTe photocathode.[66]

in a wide range: −50–100 °C, which is important, in particular, for geophysical applications.

The slow component can be strongly suppressed by the introduction into the crystal of an admixture of La (1%) (Ref. 65), as is shown in Fig. 13 (Ref. 66). The fast component is decreased by a factor of two, and the relation between it and the slow component is improved by a factor of 8 if the light is recorded by a photomultiplier with a quartz window. In Fig. 13 we also see the good agreement between the luminescence spectrum of the fast component and the spectral sensitivity of the Cs–Te photocathode, which is "blind" to sunlight.[79,88] Such a photodetector makes it possible to suppress the slow component even more effectively.

Here it is not pointless to note that even though the photomultiplier is blind to sunlight, it is better to work with it in darkness, to avoid a large rise in the noise level.

A large decrease (by an order of magnitude) is obtained when using the new K–Cs–Te photocathode, the long-wavelength limit of whose sensitivity spectrum is shifted to the left by ~30 nm in relation to the Cs–Te one (Ref. 89). In that study it is claimed that the contribution from the slow component can be decreased after 35 nsec to a level 10^{-4} by using the K–Cs–Te photocathode and a fast shaper. There are plans to develop a technology for preparing BaF_2 crystals of length 50 cm.

However, crystals with impurities are still made in small sizes. In any case, for electromagnetic calorimetry it is "pure" BaF_2 crystals without doping which are still being used. And for such a crystal a photomultiplier blind to sunlight allows the number of photoelectrons from the slow component to be lowered nearly to the number of photoelectrons from the fast component.[67]

In preparing and using a long crystal it is very important that it be uniform. In an electromagnetic calorimeter, for example, nonuniformities lead, as a result of a shower fluctuation in the longitudinal direction, to an increase of the constant term in the resolution, which at high energies can become the dominant factor.[67] The luminescence of BaF_2 in the ultraviolet imposes the corresponding difficulties on obtaining uniformity along the length of the crystal. A very important problem is the organization of the light collection in a crystal. The maximum light output is obtained if the light-collecting face is in optical contact with

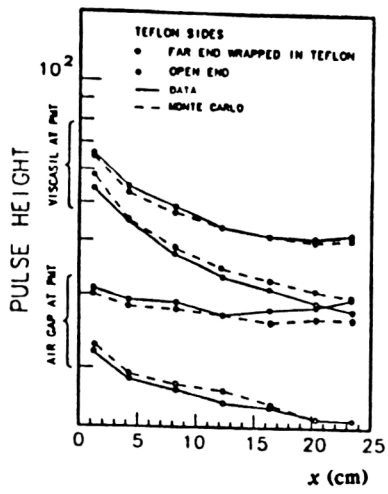

FIG. 14. Pulse amplitude as a function of the distance between the muon telescope and the photocathode of the photomultiplier for the case where the sides of the crystal are wrapped with teflon.[67]

the photocathode, while the opposite face and the sides are wrapped with teflon tape. However, this is not the best way to obtain uniformity of the crystal. The light-collection efficiency is at the very least dependent on the longitudinal coordinate if optical immersion between the photocathode and the crystal is not used. This, of course, is obtained at the cost of significantly decreasing the pulse height (by a factor of 1.5–2). In Fig. 14 we give the results of studies using a crystal of dimensions $3.6\times3.6\times25$ cm in a muon beam.[67] A muon telescope consisting of two plastic trigger counters is moved along the crystal length. The calculated curves given in Fig. 14 are in good agreement with the results of measurements for the following parameter values: 115 cm for the true absorption length, 7.5% for the optical coupling between teflon and BaF_2, and a teflon reflectivity of 95%. The partial optical coupling between

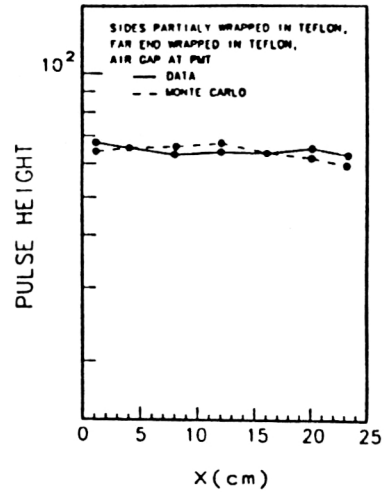

FIG. 15. Pulse amplitude as a function of the distance between the muon telescope and the photocathode of the photomultiplier for the case where the sides of the crystal and its far end are wrapped with teflon and the photomultiplier is connected with an air gap. The sides are partially wrapped.[67]

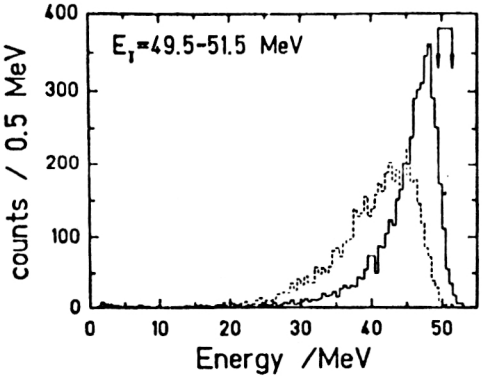

FIG. 16. Energy spectra measured using a single BaF_2 detector and a set of seven modules by summing the energies (dashed- and solid-line histograms, respectively).[90]

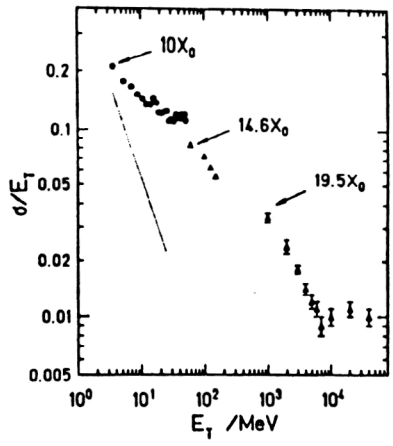

FIG. 17. Ratio of the standard deviation to the initial photon energy as a function of the photon energy for various BaF_2 detectors. The dashed line shows the effect of the spread of the photon beam.[90]

the teflon and the BaF_2 which is present is sensitive to pressure, which must be remembered when working with the detector. An even larger uniformity of the light collection was obtained with a partially unwrapped crystal: 2.2 cm at the photomultiplier end and 0.7 cm at the far end (Fig. 15). The nonuniformity from point to point did not exceed 1.5%.

The time resolution of the crystal for minimally ionizing muons was 160 psec.

Spectrometry of hard electromagnetic radiation

As already noted, the lower light yield of the BaF_2 crystal compared with NaI(Tl) at higher γ, electron, and positron energies is not decisive for the energy resolution.

The characteristics of a detector composed of seven crystals, one at the center and six surrounding it, have been studied in a beam of photons of energy 3–50 MeV (Ref. 90). The crystals were six-sided with an inner diameter of 5.2 cm and length of 20 cm, i.e., $\sim 10X_0$. Each of them was wrapped with teflon tape (the total thickness was 0.2 mm), aluminum foil (0.2 mm), and black tape (0.5 mm), and was connected with an EMI 19954 QB photomultiplier with a quartz window. Silicon paste (Baysilone 1000000, Bayer, FRG) was used. The crystals were placed right next to each other. The dead layer created by the wrapping was noticeable only at the beginning of the energy range, and at the end only $\sim$0.1 MeV was absorbed. The beam diameter was 3 cm, and the Molière radius for BaF_2 is 4.35 cm. From 80 to 85% of the initial energy was absorbed in the central crystal. The measured spectra (Fig. 16) differ noticeably from the normal distribution, being more elongated toward lower energy releases. The largest deviation was observed at $E=15$–25 MeV. Here, in addition to the usual electromagnetic interactions, a contribution of several percent can come from the (γ,n) reaction (mainly on Ba) occurring via excitation of the giant dipole resonance.

In Fig. 17 we show the energy dependence of the energy resolution, corrected for the energy spread of the primary photon beam. At the maximum energies $\sigma=10\%$. The fact that the resolution does not improve with increasing energy at the end of the energy range indicates that the detector length, equal to $10X_0$, is too short. For comparison, in Fig. 17 we also give the results of measurements for detectors of length $14.6X_0$ (Ref. 91) and $19.5X_0$ (Ref. 92); to obtain a length of $19.5X_0$ the calorimeter was composed of five crystals (Fig. 18): the first of cross section 10×10 cm, and the other four of cross section 13.5×7.5 cm. Only these four crystals were used for the length $14.6X_0$. Each crystal was attached to a three-millimeter disk of Plexiglas with an admixture of BBQ wavelength shifter (150 mg/l). An S-2575 Hamamatsu photodiode of dimensions 30×3.4 mm was attached to a section of the face. In addition to this small surface, the crystal and the disk were covered with teflon tape and then with aluminum tape. The small gap between the crystal and the shifter ensures that there is no optical contact between them. The FFC shifter plate was optimized for high light concentration on a small light-collecting area. This light concentration and the shift to longer wavelengths, where the quantum yield of the photodiode is high, made it possible to obtain twice the number of photoelectrons with it than with a photomultiplier.

The limit of the light transmission by Plexiglass is $\sim$270 nm. However, the loss of the fast component of the light in this case is insignificant, because the amplification system following the photodiode has a time constant of 2 μsec.

The energy resolution over the calorimeter length $19.5X_0$ increases up to $E\approx5$ GeV. Beyond this the resolution does not change and σ remains at the level of 1%. Roughly 0.4% comes from fluctuations in the energy leakage outside the detector for $E=40$ GeV, as shown by a Monte Carlo calculation.

For $E=5$ GeV the separation of pions and electrons was 1:500.

In Ref. 93 a detector length of $11.2X_0$ was obtained by optically connecting two crystals of cross section 12.7 $\times$11.45 cm by means of silicon oil. The two crystals were wrapped with teflon tape, aluminum foil, and black tape. Three R-2256 Hamamatsu photodiodes with quartz win-

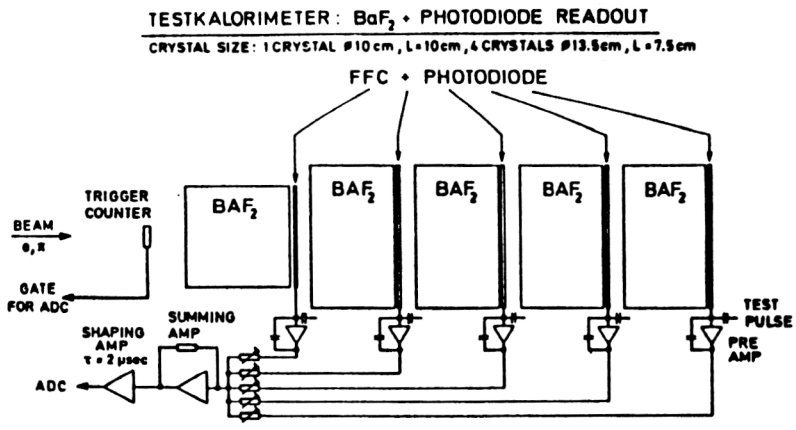

FIG. 18. Test calorimeter setup.[92]

dows of diameter 5.08 cm were attached to one face of the cylinder, using the silicone resin compound RTV. For photon energies in the range 75–200 MeV the resolution was close to that shown in Fig. 14 for a detector of length $14.6X_0$: within 10%. The shape of the spectra clearly differs significantly from a Gaussian.

From the above considerations it follows that crystals of length $\sim 10X_0$ are quite suitable for γ spectrometry for $E \leqslant 100$ MeV. Such scintillators have been used, in particular, to construct the LNS Crystal Ball multidetector spectrometer for studying pion production, which lies below the free nucleon–nucleon threshold.[94] The neutral pion decays into two photons, which are recorded in coincidence.

The Crystal Ball spectrometer is made as a 4π setup in order to detect both hard photons and charged particles. It can be used to record events in which all the secondary particles are observed by measuring their energy and emission angle. This favorably distinguishes this type of detector from detectors based on lead glass, which record only γ quanta from their Čerenkov radiation. The energy resolution of a Čerenkov detector is considerably worse, although the absence of Čerenkov radiation ensures strong background suppression.

A 4π system made of 180 BaF_2 crystals, also designed to record γ rays and light charged particles, is described in Ref. 95.

Dependence of the shape of a scintillation on the type of radiation

The ionization density affects both the ratio of the intensities of the luminescence of the fast and slow components in BaF_2, and also the duration of the latter component. In measurements with 5–6 MeV α particles the fast component was practically not observed.[96] The slow component itself consists of two components: the main one with luminescence time $\tau_1 \approx 600$ nsec and an additional one with $\tau_1 \leqslant 100$ nsec, the duration and intensity of which depend on the type of radiation, as can be seen in Table IV (Ref. 96).

It is possible to discriminate γ quanta (electrons) from other particles according to the shape of the scintillation.[97,98]

Particles with different ionization density are discriminated by using the difference between their light outputs of the fast component E_{fast}. Great progress in particle discrimination was achieved by using the procedure on which the "constant-fraction" time technique is based to analyze the signal.[99] Here a bipolar pulse, the point of intersection of which is independent of the energy absorbed in the crystal, is formed. The first part of the momentum is proportional to E_{fast}. In Fig. 19 we show the two-dimensional E_{fast} versus E_{tot} (the total energy) spectrum measured in the reaction $^6\text{Li} + ^{12}\text{C}$ for bombarding-ion energy 36 MeV, using a BaF_2 crystal of volume 350 cm^3. Proton and deuteron events are discriminated beginning at 6 MeV. This has not been observed in obtaining E_{fast} from monopolar pulses.

Good discrimination of p, d, t, and α in that study was obtained by the $(\Delta E$–$E)$ technique, using a 50 μm-thick silicon ΔE detector. The introduction of the ΔE detector naturally gives rise to some threshold, which imposes a corresponding constraint on the use of this technique.

Particle discrimination can be improved significantly

TABLE IV. Luminescence time and intensity of the slow component of BaF_2 for various particles.

Type of particle	Luminescence time (nsec)		Intensity ratio I'/I
	τ_1	τ_1'	
Electrons	600±60	100±2	0,06±0,02
α-particles	550±50	50±10	0,11±0,02
Fission fragments	580±30	9±2	0,08±0,02

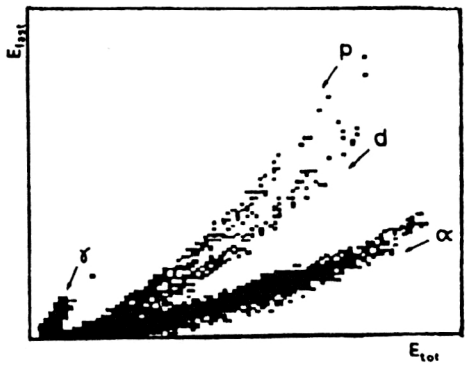

FIG. 19. Two-dimensional $E_{\text{fast}}-E_{\text{tot}}$ spectrum (Ref. 99).

by using the time-of-flight technique in conjunction with data on E_{fast} and E_{tot}. The results of such measurements in the detection of 8–130 MeV photons by a crystal of cross section 10×14 cm are given in Ref. 100, and those for a beam of ^{40}Ar ions and a crystal of length 10 cm and diameter 31.5 mm are given in Ref. 101.

The spectrum of secondary particles emitted at an angle of 10° in the $^{40}\text{Ar}+^{27}\text{Al}$ reaction at 58 MeV/nucleon was measured in a recent study. The time of flight $(t-t_0)$ was measured on a base of 1.2 m. The time resolution was 600 psec from ^{60}Co, and the energy resolution was $\approx 11\%$ (^{137}Cs). The two-dimensional $[E_{\text{fast}},E_{\text{tot}}]$ and $[(t-t_0),E_{\text{tot}}]$ spectra could be used separately to discriminate particles only for $Z=1$ and $Z=2$. The function $I=E_{\text{fast}}/[E_{\text{tot}}(t-t_0)^2]^{\alpha}$ was used for particle identification. The parameter $\alpha=1/2$ was determined empirically.

This function is shown in Fig. 20 as a function of the total energy. Good particle discrimination up to $Z=3$ and $A=7$ is seen. The use of the time-of-flight technique in a particular experiment is restricted by the need to have a definite base for the particle path and an accurate starting signal.

The search for ways to lower the detector cost

The photomultipliers with quartz windows used to record ultraviolet light from BaF_2 monocrystals are expensive. To understand how cheaper ordinary photomultipliers can be used, a number of shifters which reemit light at longer wavelengths have been studied. A layer of p-terphenyl of thickness ~ 1 mg/cm^2 was deposited on a crystal of cross section 5×5 cm. An energy resolution of 13.7% for ^{137}Cs and a time resolution of 300 psec for $(\gamma-\gamma)$ coincidences from ^{60}Co (1.17 and 1.33 MeV) were obtained (Ref. 97). Without the shifter these resolutions were 12.6% and 165 psec, respectively. When the layer thickness was increased to 2 mg/cm^2 the energy resolution was even observed to improve by 1–1.5%, but the time resolution went down by a factor of two compared with the case without the shifter.[102] Nearly the same improvement of the energy resolution and worsening of the time resolution was obtained when using a shifter of p–p'-diphenylstilbene.[103] The use of this shifter on a long crystal of dimensions $3.2\times3.2\times15.0$ cm was accompanied by a change of the energy resolution from 7.5% to 10% and of the time resolution from 0.3 nsec to 0.5 nsec (Ref. 104).

The fast time characteristic of the detector was nearly preserved when use was made of liquid scintillators based on toluene of the type ZhS-67 or ZhS-70, which emit light with a maximum at $\lambda=380$–390 nm, with a luminescence time $\tau=0.6$–0.7 nsec (Ref. 105).

The index of refraction of the organic scintillators used as shifters is close to the index of refraction of BaF_2. This made it possible to obtain from these materials sufficiently optically uniform solid[106,107] and liquid[108] mixtures.

The same light yield as for BaF_2 was obtained with a mixture of 70–86% BaF_2 powder and methylmetacrylic resin with the addition of 0.02% BDB, which emits light with maximum at $\lambda=410$ nm. A heavy plastic scintillator with good mechanical properties was obtained, but the energy resolution of this plastic was worse by a factor of two than that of the monocrystal. For $E<110$ MeV good separation of α, p, and γ was obtained by using the two-dimensional $(E_{\text{tot}},E_{\text{fast}})$ spectra. Two organic scintillators turned out to be suitable for the liquid mixture (a gel). The first is toluene+methanol+PPO+POPOP, which has index of refraction $n=1.487$ for $\lambda=254$ nm; the index of refraction of BaF_2 at this wavelength is $n=1.5122$. The gel has a light yield 1.5 times higher than BaF_2, and its cost is an order of magnitude less. The other variant uses decalin +PPO+POPOP. The radiation length of the gel is 2.8 cm. The signal is short—several nanoseconds—but has a long tail. The optical length of light absorption is still small, 30 cm, and the resolution is not yet satisfactory.

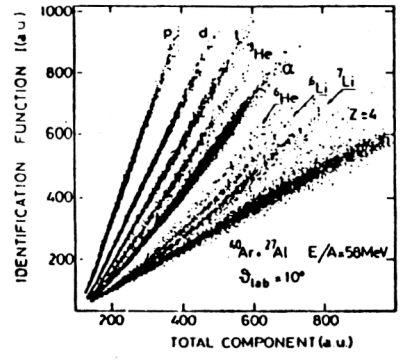

FIG. 20. Identification function I (see the text) as a function of the full component.[101]

6. RADIATION STABILITY OF DETECTOR MATERIALS

NaI(Tl) can be used in a γ flux of density up to 10^5 photons/(sec·cm^2) without significantly changing the characteristics. Loss of light of the scintillation occurs as the flux increases. For fluxes above 10^7/sec the changes in the characteristics become irreversible.[109] This mainly occurs owing to loss of transmission of the intrinsic radiation. At a dose of 110 rad/h from ^{241}Am and at room temperature the signal amplitude fell by about 40% during about an hour, and then did not change. It has been shown[110]

that for crystals with lower dopant concentration the light yield is decreased less, and so the resolution does not become as bad. Increase of the working temperature by 40–50° above normal significantly (by a factor of 2 to 3) decreased the worsening of the intrinsic resolution of detectors subjected to γ radiation.

It is now well known that annealing allows NaI(Tl) crystals damaged by radiation to be restored to a large degree.

The data given in Ref. 111 indicate a smaller radiation damage to a NaI(Tl) test crystal of cross section 2.5×152 mm. A 400-rad dose from ^{60}Co caused the signal amplitude to fall by $\sim 18\%$. For a CsI(Tl) crystal the same dose caused the signal amplitude to fall by a factor of two. In Refs. 111–113 a significant decrease of the amplitude was seen for even a 100-rad dose. An increase of the afterglow was also observed.[112] It turned out that the light output depends strongly on the crystal dimensions. In a small cubic crystal with linear dimension 2.5 cm the light output does not decrease up to doses of 800 rad from ^{60}Co (Ref. 19). More damage was seen in crystals grown from purer materials, which may explain the discrepancy in the results obtained by different authors. Larger crystals of dimensions $5\times 5\times 30$ cm were exposed to a 100-rad dose for 20 minutes, twice during 20 days. Some of these crystals were distinguished by the fact that they phosphoresced for several hours after exposure to daylight. In such crystals the light output was decreased by ~ 15–35% and did not change with time. In crystals without phosphorescence the decrease in the first exposure was about 10% and somewhat smaller in the second. Then the process of restoration of the light output occurred. In two of the three crystals the light output reached its original value after 70 days. This process can be accelerated by annealing. The measurements did not reveal any difference between cases where the total radiation dose of 100 rad was received over 20 minutes or over 72 hours.

The problem of afterglow of a sample prepared from particularly pure CsI(Tl) did not arise after irradiation.[114] During irradiation of a crystal the impurities form color centers, which considerably decrease the scintillation light. It has been found that the absorption increases with decreasing wavelength of the light and mainly appears for $\lambda < 600$ nm. Incidentally, this fact makes photodetectors with spectral sensitivity strongly shifted to the right, i.e., solid-state photoanodes, better than photomultipliers.

Since the main consequence of irradiating a crystal is some loss of its transmission, the signal amplitude will depend on the crystal dimensions. The results of measurements for a CsI(Tl) crystal of length 10 cm are given in Ref. 114. For a dose of 1.58×10^3 rad the amplitude decreased by 28%. It was to a large degree restored after several hours of exposure to daylight.

"Pure" CsI has a radiation strength an order of magnitude larger than CsI(Tl) (Ref. 104).

Fairly extensive radiation damage to phosphorescent crystals has also been observed for BGO (Ref. 115). In this crystal the radiation stability depends strongly on the crystal dimensions. For example, for linear dimensions of up to 30 mm a dose of 3.6×10^6 rad from ^{60}Co led to only a slight darkening of the crystal, which half disappeared several days after the irradiation stopped and completely disappeared after a much longer period.[116] The change in the scintillation efficiency of the crystal was much smaller than the change of its optical transmission. The crystal was also bombarded with a 10^6-rad dose of 12-GeV protons and fast neutrons. It was found that these types of radiation affect BGO an order of magnitude more strongly than low-energy γ rays.

After bombardment with an 8×10^7-rad dose of γ rays, a crystal of cross section 25×25 mm lost 32% of its optical transmission; 85% of this transmission was restored after 24 hours.[117]

A decrease of the light yield by 10–20% was observed in long crystals (10–24 cm) starting at doses of hundreds of rads.[111,118] The weakening of the light was large at $\lambda = 400$–600 nm. Spontaneous restoration of the crystal transmission occurred, but only after many days.

The change of the light yield of a crystal induced by radiation varies from sample to sample. It depends on the impurities in the sample. Study of the correlation between the radiation defects in BGO and impurities in the crystal showed that three groups can be distinguished according to the strength of the effect.[119] Each of these groups occupies its own radiation-induced absorption band. Their energy levels lie above the valence band by (2.3 ± 0.1), (3.0 ± 0.1), and (3.8 ± 0.1) eV. Cr, Mn, Fe, and Pb form the first level, Al, Ca, Cu, and Si form the second, and Co, Ga, Mg, and Ni form the third. The elements of the first group, which are closest to the valence band, lead to the largest radiation damage. The elements of the second zone are located relatively far both from the valence band and from the conduction band, and their effect is negligible. The third group has an intermediate effect. The special role of iron as an impurity is shown in Ref. 120, in which several crystals were studied for increasing doses from ^{60}Co. Optical absorption mainly appeared in the blue region and was a consequence of the formation of color centers. The absorption grew linearly as the dose increased to several rad, and then, beginning at 10^4 rad, it entered a plateau (Fig. 21). It was suggested that the saturation reflects the fact that all the defects are occupied by captured charges. Color centers from yellow to brown shades were formed after irradiation with a 1-krad dose. Already at room temperature the thermal energy was sufficient for the spontaneous restoration of BGO crystals. A restoration of 60–70% was observed after 100 hours. However, there were some crystals which at room temperature were almost not restored at all. The restoration process accelerates as the temperature is raised.[118] Two hours were sufficient to restore a crystal at 160 °C.

The introduction of Eu into a BGO crystal significantly improves its radiation characteristic.[121] Crystals of dimensions $25\times 25\times 50$ mm were irradiated with a dose of 1–10 krad, which worsened the transmission and the resolution. However, for BGO(Eu) the subsequent restoration of the crystal characteristics was much faster. The fluorescence spectrum in this crystal is shifted to the right.

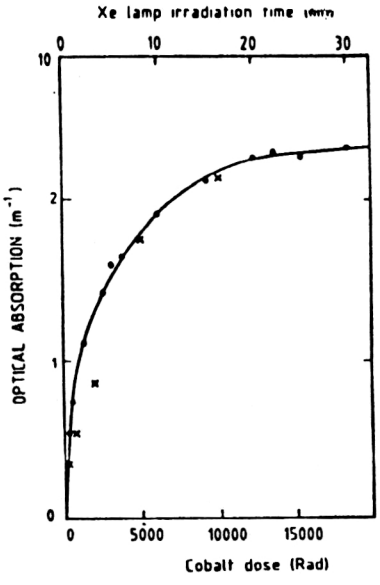

FIG. 21. Total absorption in the range 400–600 nm as a function of the total dose for (●) ultraviolet light (a 320-nm xenon lamp) and (×) a cobalt source.[120]

A defect of BGO(Eu) is the presence of a 3 msec-long afterglow with an amplitude of several percent.[120]

After BGO was irradiated by 1.5-GeV protons for a total dose of 1.1×10^8 cm^{-2} over two days, the energy resolution worsened by only 70%, but the background from the crystal itself increased considerably.[122] This was mainly attributable to the increased radioactivity of bismuth. Under extended work in this beam equality between the production and decay of the crystal's own radioactivity was established over the course of one week. This background is not a big problem if the measured energies are large, as in the case where BGO is used for electromagnetic calorimeters.

Studies of the radiation hardness of BaF_2 have been carried out for crystals of small dimensions. Crystals 4 and 6 mm thick were bombarded by an 800-GeV/c proton beam (Ref. 123). The scintillation yield did not decrease up to a dose of 1.3×10^7 rad, and only a small decrease of the transmission was observed.

After an 8×10^7 rad-dose of β and γ radiation, the transmission of a crystal of cross section 2.5×2.5 cm decreased by 4% at 250 nm and was restored after a day.[117]

A shortening of the optical attenuation length of light in crystals of dimensions $20\times10\times1$ mm by 14% after a 10^7-rad dose of γ rays was reported in Ref. 66. The defects were comparable to those observed for BGO. It is assumed that the presence of impurities is an important factor in radiation damage.

The effect of radiation from α particles of energy 5.6 MeV and protons of energy 1.5 MeV has been studied for a $1.5\times1.5\times1$ cm crystal.[98] A 20% decrease of the pulse amplitude was observed for doses of 2×10^{14} and 7×10^{14} particles/cm^2, respectively.

The losses of optical transmission of a 12 mm-thick crystal after irradiation with a dose of 1.15×10^7 rad from ^{60}Co were mainly for $\lambda<170$ nm, and at $\lambda=220$ nm they were 10% (Ref. 124). Practically no restoration was observed.

The content of uncontrollable impurities in a crystal which is irradiated mainly affects the decrease of its transmission in the short-wavelength region. The content of such impurities can vary significantly from sample to sample. However, it is not only a loss of transmission which leads to a decrease of the signal amplitude. According to the data of Ref. 124, the decrease of the transmission at $\lambda=250$ nm after irradiation with a dose of $\sim10^6$ rad was 10–15%, while the light yield decreased by 30%. The dependence of the light yield on the integrated dose of γ rays from ^{60}Co is shown in Fig. 22 (Ref. 125). The rapid falloff for doses of up to 10^6 rad is seen, and then up to 10^7 rad the change is very smooth. No dependence on the rate at which the dose was obtained was discovered. For the maximum dose the energy resolution worsened from 12.8% to 16%. It was almost completely restored after 10 hours of exposure to sunlight.

Scintillators are usually connected to photodetectors by a thin (up to ~10 μm thick) layer of optical glue. The

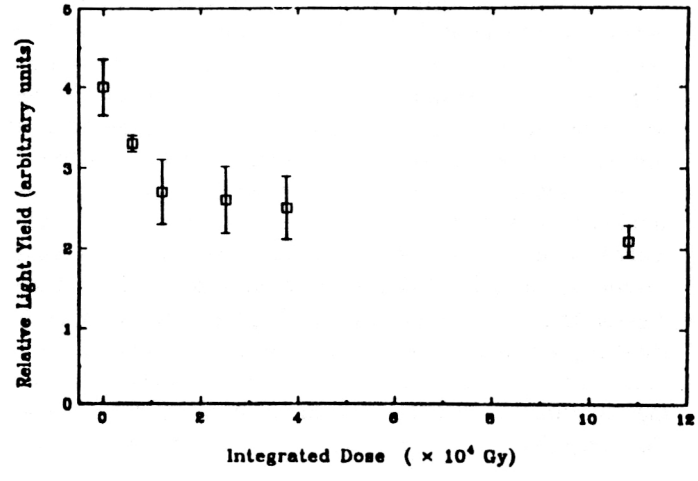

FIG. 22. Light output as a function of the integrated dose of γ rays for BaF_2 (Ref. 125).

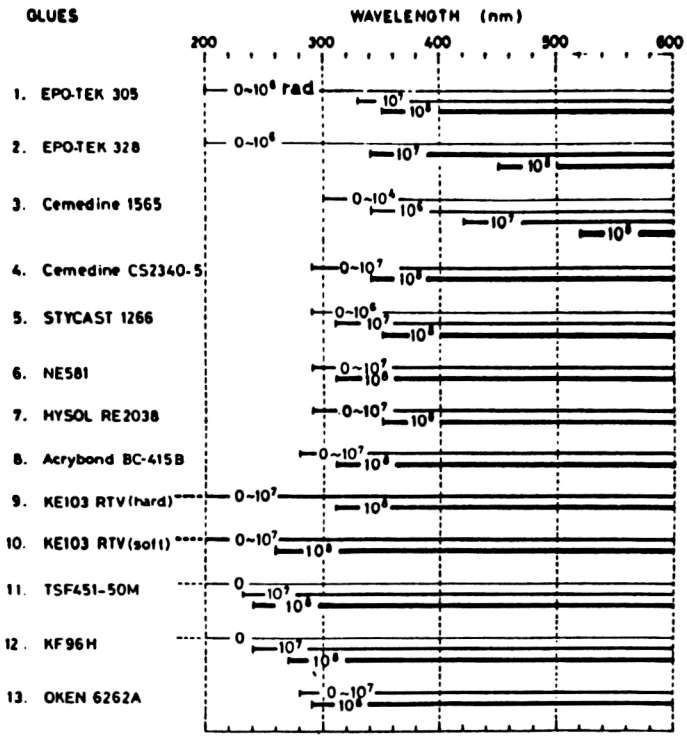

FIG. 23. Radiation strength of optical glues. Each line with the cumulative dose gives the wavelength range in which the glue satisfies two criteria (see the text) for it to be used successfully in calorimeters.[126]

radiation damage of a series of adhesives exposed to γ radiation from ^{60}Co has been studied.[126] Layers of glue were placed between two quartz plates, the transmission of which began to change only for a dose of $\sim 10^8$ rad. The optical transmission in the wavelength range 200–600 nm was measured by a spectrophotometer. Naturally, the effect of radiation defects increased with decreasing λ. The suitability of each glue for a certain range of λ was determined according to two criteria: 1) For λ_{min} the transmission must be greater than 50%; 2) the allowed dose is taken to be that for which the loss of transmission is less than 10%. The results of the measurements based on these two criteria are shown in Fig. 23.

In conclusion, we should note that at doses of $\sim 10^8$ rad a problem must also arise with the photodetectors, particularly solid-state ones.

7. FAST HEAVY SCINTILLATORS

Cerium fluoride

Cerium fluoride CeF_3 has two luminescence components: $\tau_1 = 5$ nsec and $\tau_2 = 30$ nsec with total intensity roughly the same as that of the fast component of BaF_2 (Refs. 127–129). In Ref. 5 the light output was 46% of that of BGO and $\tau_2 = 20$ nsec.

The time and energy resolution of CeF_3 must be worse than those of BaF_2, but the flux which can be handled is many times larger. Its radiation length is $X_0 = 1.7$ cm, i.e., smaller than that of BaF_2 (2.1 cm). The crystal is nonhygroscopic, and its index of refraction is $n = 1.68$ An important advantage of CeF_3 is the possibility of working with cheaper photomultipliers not containing quartz. The peak emission for the fast component is at $\lambda = 300$ nm, and that for the slow component is at $\lambda = 340$ nm. Moreover, in Ref. 130 the emission peak occurs at 375 nm. The authors of that study investigated the radiation strength of a CeF_3 crystal of dimensions $7 \times 7 \times 35$ mm. A dose of 10^7 rad induced a degradation of less than 5% per unit radiation length. The properties of the crystal were restored with a time constant of 40 days. When the dose was increased to 10^8 rad, the degradation rose to 19%. It seems that CeF_3 has greater radiation stability than BaF_2.

Gadolinium orthosilicate

The pure Gd_2SiO_5 (GSO for short) monocrystal itself is a scintillator. However, its light yield is small and increases to 20% of the light yield of NaI(Tl) when a 0.5–5% admixture of cerium is added to it (Refs. 131–133). Here the luminescence time of GSO:Ce varies from 60 to 30 nsec. But for a large concentration of Ce the crystal acquires a brownish shade. Two luminescence components were seen in Ref. 133: the main one, $\tau_1 = 56$ nsec, and another, $\tau_2 = 600$ nsec, at the 10–15% level. The emission peak of the crystal is located at $\lambda = 440$ nm, i.e., in the region of the maximum sensitivity of ordinary photomultipliers. The crystal is nonhygroscopic, and its index of refraction is $n = 1.85$. The radiation length $X_0 = 1.38$ cm is smaller than that of CeF_3. Whereas for CeF_3 the attainable length at present does not exceed $3X_0$, in Ref. 134 measurements for a GSO:Ce crystal of length $14.2X_0$ and diameter 4.9 cm are described. This crystal in a 1-GeV electron beam had a resolution of 7% (FWHM). The e/π separation for particles analyzed according to their momentum was 1:1000 for an energy cutoff of $\pm 2\sigma$ at the electron peak.

TABLE V. Pulse-height ratio (PHR), resolution for E_γ=662 (FWHM), pulse rise time T (10–90%), number of unit charges produced in a 1-MeV loss (e–h pairs/MeV), and energy consumed in the production of a unit charge in the photodiode in irradiation by γ rays ($E_\gamma/(e$–$h)$ pair).

Type of scintillator	Height H, mm	With photomultiplier			With photodiode			$E_\gamma/(e$–$h)$ pair
		PHR	FWHM, %	T (10–90%) μsec	PHR	FWHM, %	e–h pair/MeV	
NaI(Tl)	20	100	7,07	0,5	100	16,8	12300	81,0
CsI(Na)	7	122	7,37	4	169	22,5	20900	47,9
CsI(Tl)	7	78	5,66	4	291	7,64	35900	27,8
GSO:Ce	10	28	7,82	0,1	47	29,3	5860	170,8
$CdWO_4$	20	21	7,97	20	53	31,8	6580	152,0
BGO	10	17,5	9,05	0,8	41	40,8	5070	197,4
BaF_2	20	13	11,37	3				

GSO:Ce surpasses all other scintillators in radiation stability. It can operate up to doses of at least 10^8 rad. However, GSO:Ce is an expensive crystal. It costs twice as much as CeF_3 and BGO.

8. COMPARISON OF SCINTILLATOR CHARACTERISTICS

The amplitude characteristics of a number of scintillators measured using the same Hamamatsu R-1306 photomultiplier and a silicone diode are given in Table V (Ref. 16). The area of the crystals matched the photodiode area (1 cm^2, Hamamatsu S-190-02), and their height H is given in the table. The small dimensions of the crystals ensured the most favorable conditions for the light yield and crystal resolution.

Measurements were carried out with the photomultiplier in photodiode mode in order to determine the absolute number of photoelectrons. Here the network and the first and second dynodes were joined together and connected to a charge-sensitive preamplifier. The scintillation efficiency of NaI(Tl), CsI(Tl), and CsI(Na) crystals was 11.9, 12.3, and 12.7%, respectively.

The maximum amplitude of the signal from the photomultiplier was obtained for CsI(Na) and NaI(Tl). However, the resolution of these crystals was better than that of CsI(Tl).

For $E_\gamma < 100$ keV the best resolution was that of CsI(Na), which was the same as that of CsI(Tl) and NaI(Tl), as is illustrated in Fig. 24.

It can be assumed that the resolution of these crystals for $E_\gamma > 100$ keV was affected by the individual features of the specific detectors. In fact, for example, for NaI(Tl) the resolution at 662 keV given in Ref. 7 is considerably better. A resolution of 5.6% was obtained for a crystal of larger size (cross section 25×25 mm). In most cases better resolution with photomultipliers is still obtained by using NaI(Tl).

The advantages of the CsI(Tl) crystal are certain when the photodetector is a solid-state photodiode. The resolution in this case for various types of crystal is shown in Fig. 25 (Ref. 16). A resolution of FWHM=5.6% for 662-keV γ rays was obtained for CsI(Tl) connected to a photodiode.[135]

In Fig. 26 we show the values of the energy resolution at different energies obtained in using a CsI(Tl) crystal with an avalanche photodiode (APD) and silicon and HgI_2 photodiodes of area 1″×1″, and also a NaI(Tl) crystal with a photomultiplier.[170] The figure shows the improvement of the resolution for $E \leqslant 1$ MeV as a result of the

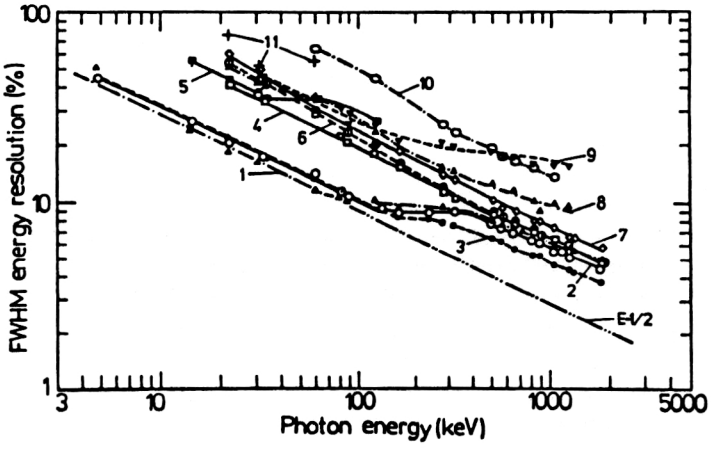

FIG. 24. Energy resolution, as a function of the photon energy, obtained in a Hamamatsu R1306 photomultiplier with a double-alkali photocathode with the following crystals: (1) 10×10×7 mm CsI(Na); (2) 10×10×20 mm NaI(Tl); (3) 10×10×7 mm CsI(Tl); (4) 10×10×10 mm GsO:Ce; (5) 10×10×20 mm CaF_2(Eu); (6) 10×10×10 mm $CdWO_4$; (7) 10×10×10 mm BGO; (8) 10×10×20 mm BaF_2; (9) 10×10×20 mm CsI ("pure"); (10) 10×10×20 mm NaI ("pure"); (11) 10×10×6 mm Ne905 Li-glass scintillator (Ref. 16).

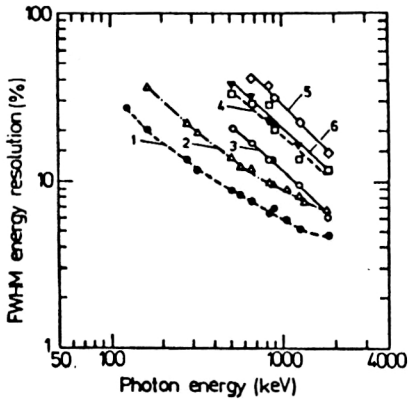

FIG. 25. Energy resolution as a function of the photon energy, obtained using a silicon photodiode (Hamamatsu S-1790-02) with the following crystals: (1) $10\times10\times7$ mm CsI(Tl); (2) $10\times10\times7$ mm CsI(Na); (3) $10\times10\times20$ mm NaI(Tl); (4) $10\times10\times10$ mm GsO:Ce; (5) $10\times10\times20$ mm $CdWO_4$; (6) $10\times10\times10$ mm BGO (Ref. 16).

introduction of amplification (APD) into the silicon photodetector. However, better results at low energies are still obtained by using other photodetectors: an HgI_2 photodiode and a photomultiplier. With an APD at $E=662$ keV the resolution was 6.9%. The resolution for this energy was improved to 4.4% by using an APD of diameter 1 cm cooled to 260 K, which is a record result.

Beginning with energies of several MeV and higher, the resolution still to a large extent depends on the crystal size, owing to energy leakages to the outside. Such a characteristic as the radiation length X_0 becomes important. The smaller X_0 is, the more compact the detector. BGO has the minimum X_0. The value of X_0 is shown in Table VI together with other characteristics of various scintillators. Crystals of length $\sim 20X_0$ and above are required for electromagnetic calorimeters for $E>100$ GeV. At present this requirement is satisfied by NaI(Tl), CsI(Tl), CsI, and BGO.

Another requirement, that of high radiation stability of the crystal, is becoming more and more important. BGO is better in this characteristic than cesium and sodium iodide, but BaF_2 is best. The presence of a fast component in the light emission of BaF_2 makes it possible to obtain the same time resolution as with a plastic scintillator, although owing to the slow component the speed of response of a detector with such a crystal is small. BaF_2 has been widely used up to moderately high energies.

Undoped CsI is almost as fast as plastic scintillators, but its radiation stability is better than that of both BaF_2 and BGO. The faster crystal CeF_3 is not as good as BaF_2 in its radiation stability. The highest radiation stability is that of the fast crystal GSO:Ce. This crystal is the most expensive.

The separation of electrons and hadrons must improve as the ratio X_0/Λ_I decreases. It is a minimum for BGO, compared with which this ratio for CsI is almost the same, while for BaF_2 it is 40% higher.

The linearity of the light output of a crystal as a function of the energy of the recorded radiation is limited by losses to luminescence at high ionization density. The smallest deviation from linearity should be expected for the largest α/β ratio. It is a maximum for cesium iodide (see Table VII). The results of its measurement for CsI(Tl) depend, as was shown in Ref. 23, on the time constant of the signal shaping. The α/β ratio decreases as this constant increases to a value of 10 μsec, at which it is ≈ 0.56, i.e., about the same as for CsI(Na). The characteristics of BGO for strongly ionizing particles are close to those of CsI(Tl) (Fig. 10) (Ref. 36). The α/β ratio is considerably smaller for BaF_2.

The dependence of the light yield on the ionization density can, in particular, be a source of nonlinearity in electromagnetic calorimeters at superhigh energies, when a large number of slow particles is formed.

In γ spectroscopy for $E_\gamma \lesssim 10$ MeV neutrons are usually the main background radiation. Here an important characteristic is the cross section for thermal-neutron capture, which is given in Table VII for the basic scintillation detectors. It is a minimum for BaF_2. However, the neutron detection mechanism in detectors is not limited to only radiative capture of neutrons slowed to thermal energies.[136] This is particularly clearly seen with a detector based on lead glass, for which the capture cross section is only 0.3×10^{-24} cm^2. The measurements of Ref. 137 showed

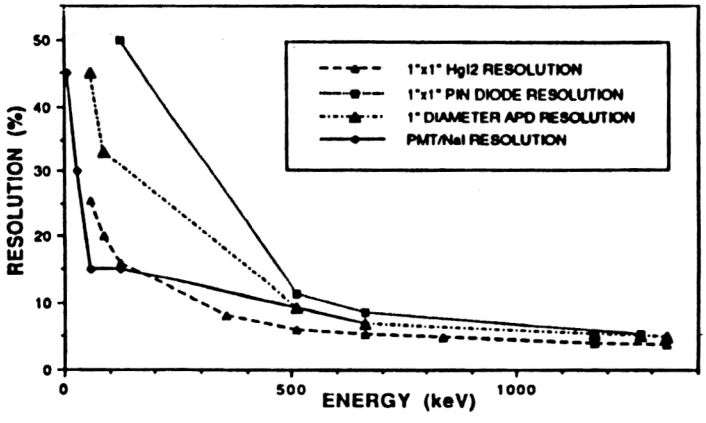

FIG. 26. Comparison of the resolution as a function of energy for several different types of scintillation detector.[170]

TABLE VI. Properties of a number of scintillating monocrystals.

Crystals / Characteristics	NaI(Tl) [15]	CsI(Tl) [15]	BGO [15]	BaF_2 [134]	CsI [134]	CeF_3 [134]	GSO:Ce [134]
Density, g/cm^3	3,7	4,51	7,13	4,9	4,53	6,16	6,71
Radiation length X_0, cm	2,59	1,86	1,12	2,1	1,86	1,7	1,38
Luminescent time, nsec:							
fast				0,6	10	30	30—60
slow	230	900	300	620	10^3		
Peak emission, nm:							
fast				220	305	375	440
slow	415	550	480	310	400		
Index of refraction*	1,85	1,8	2,15	1,56	1,8	1,68	1,85
Relative light output:							
fast				5	4	4—5	20
slow	100	45	10—20	16	4		
Hygroscopicity	yes	slightly	no	no	small	no	no
Radiation stability (Ref. 134), rad	10^3	10^3 [114]	10^{5-6}	10^{6-7}	10^{4-5}	10^{6-7}	10^8
Nuclear interaction length, cm	41,3	36,4	23	21,4	[17]		
X_0/Λ_I	0,063	0,051	0,049	0,069			
Molière radius, cm	4,3	3,8	2,7	4,35	[90]		
Attainable length X_0	20	20	20	10—15	20	3	13
Price (Ref. 134), \$/cm^3	1—2		10—12	7—8	1—2	10	20—25

*According to Ref. 67, for BaF_2 at $\lambda = 220$ nm, $n = 1.63$.

that for this detector the neutron detection efficiency is close to that of scintillators. The contribution of the background radiation decreases with decreasing detector volume, which is usually specified by using the γ detection efficiency. For a given γ efficiency BGO has linear dimensions nearly half those of other crystals, so that the contribution of the neutron background can be decreased accordingly.

9. FURTHER IMPROVEMENT OF INDIVIDUAL TYPES OF SCINTILLATOR

BGO crystals prepared using the new version of the Bridgman technology have proved to be significantly more stable to radiation than crystals grown by other methods.[138] The optical transmission of a crystal of dimensions $2.5\times2.5\times1$ cm after irradiation with a 130-Mrad dose was degraded by no more than 10%. Annealing of the crystals at 400 °C in air for two hours restored the original transmission. The crystals remain colorless after exposure to ultraviolet light or daylight. Meanwhile, crystals prepared by other methods yellow.

As mentioned above, the BGO crystal became considerably more stable to radiation when it was doped with Eu (Ref. 121). However, then afterglow appeared (after 3 msec). The properties of BGO doped with Ce, Pr, Tb, and Yb were studied in Ref. 139. The results were best when the latter was used. The absorption and emission spectra of BGO(Yb) are shown in Fig. 27. Their clear separation

TABLE VII. Additional characteristics of scintillating materials.

Crystals / Characteristics	NaI(Tl)	CsI(Tl)	CsI(Na)	BGO	BaF_2
α/β [65]	0,5	0,8 0,7 [20] 0,56 [23]	0,58		0,34
Cross section for thermal neutron radiative capture(10^{-24} cm^2) by a molecule of the scintillator material.[136]	6,7	35		7,1	1,2

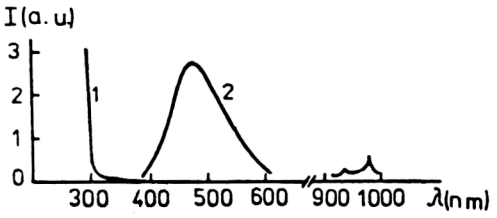

FIG. 27. Absorption (1) and emission (2) spectra of BGO(Yb) (Ref. 139).

makes it possible to obtain BGO(Yb) crystals greater than 20 cm in size of practically the same transmission as "pure" BGO. The introduction of Yb into the crystal leads to a significant curtailing of its light emission (Fig. 28). There is a luminescence component with $\tau=16$ nsec which gives a 16% contribution for a 1% concentration of Yb (by weight). The value of the contribution of the fast component is correlated with the dopant concentration, but at large concentration afterglow appears.

The BGO(Yb) crystal is distinguished by its high stability to radiation. The authors of Ref. 140 quote the same value of allowed dose for it as for GSO:Ce, but BGO(Yb) is considerably cheaper.

The slow component of the luminescence of BaF_2 greatly restrains the use of this crystal when the radiation flux is high, although the radiation stability of this crystal is relatively high.

It is expected that this difficulty will be overcome by using new photodetectors whose spectral sensitivity lies in the ultraviolet region, not including the luminescence spectrum of the slow component. The technology of preparing BaF_2 crystals for the purpose of increasing their length to $20X_0$ is being perfected.

There has been considerable progress in growing CeF_3 crystals of large size; their high radiation stability and operating speed make them attractive for electromagnetic calorimetry at modern colliders.[5]

It should be noted that the radiation stability of the CeF_3 crystal was raised by another order of magnitude by the introduction of BaF_2 (0.67%) into it (Ref. 141). Whereas a dose of 1.2×10^7 rad led to an 11% decrease of the transmission of "pure" CeF_3 at $\lambda=340$ nm (the emission peak), no such decrease was observed for CeF_3:BaF_2. It was small after a dose of 10^8 rad. Tests were performed on samples of diameter 1 cm and thickness 5 mm. CeF_3:BaF_2 has a light output of 82.3% relative to "pure" CeF_3 and a luminescence time of $\tau=28.3$ nsec.

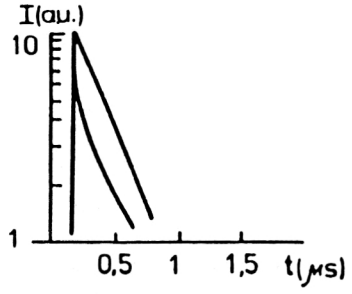

FIG. 28. Scintillation kinetics of BGO(Yb) (lower curve) and "pure" BGO (upper curve) (Ref. 139).

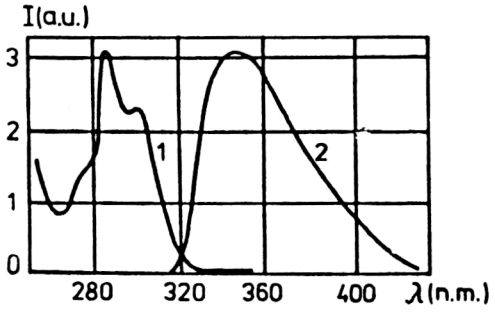

FIG. 29. Absorption (1) and emission (2) spectra of $YAlO_3$ crystals. The crystal thickness is 1 mm, and the temperature is 300 K (Ref. 143).

10. THE SEARCH FOR PROMISING NEW SCINTILLATION DETECTORS

Yttrium–aluminum oxides

$Y_2Al_5O_{12}$ crystals (garnet) and $YAlO_3$ (perovskite, YAP) are well known in laser technology. By doping them with cesium (0.1–1.0% by weight) they can be made into scintillators. $Y_2Al_5O_{12}$:Ce has a light yield of the order of 4% of that of NaI(Tl), $\tau=70$ nsec, and $\lambda_{max}=550$ nm (Ref. 142). The light yield of $YAlO_3$:Ce for a concentration of CeO_2 of 0.2% by weight is 40%, $\tau=28$ nsec, $n=1.93$, and $\lambda_{max}=347$ nm (see Fig. 29) (Ref. 143; the value $\lambda_{max}=390$ nm is quoted in Ref. 5). The luminescence time can be decreased by another factor of two by additional doping with Yb ions (1% by weight), but here the light yield falls to 6%. Monocrystals of high optical quality of dimensions $8\times10\times1.5$ cm have been obtained for which the resolution at the α line of ^{226}Ra of energy 7687 keV is 2.5% (FWHM).

The crystals are nonhygroscopic, chemically stable, and possess good mechanical properties. This makes it possible to prepare samples of the small thickness (50–100 μm) needed for low-background α spectrometers.

A distinctive feature of YAP is the preservation of the linear dependence of the light output on energy at large ionization density. In the α-particle energy range 5.8–8.4 MeV the linearity was preserved within ±2% (Ref. 144).

The light output also depends weakly on the cerium concentration. As the CeO_2 concentration is varied from 0.1% to 1% the light output increases by 30%. The weak dependence of the light output on the ionization density and dopant concentration is a valuable quality of crystals, particularly in multidetector systems. The temperature coefficient of YAP is 0.39%/K.

Large numbers of tiny ($3\times3\times0.1$ mm) YAP crystals have been used to calibrate calorimeter photomultipliers from α particles (Ref. 144). The radiation resistance of YAP is very high, $\sim10^8$ rad (Ref. 145).

TABLE VIII. Characteristics of heavy scintillators.

Type of scintillator	d, g/cm^3	I, %	λ, nm	τ_1, nsec	I_1, %	τ_2, nsec	I_2, %	τ_3, nsec	I_3, %
BGO	7,13	100	480	300	100				
CdF_2	6,6	13,3	420	4,8	29	24	28	78	43
2 ($PbCo_3$)—$Pb(OH_2)$	6,7	8,0	475	5,6	24	25	48	155	28
HfF_4	7,1	3,7	350	29	100				
$PbWO_4$	8,2	3,6	490	2,5	25	11	29	98	46
$PbCl_2$	5,9	28	500	2,9	41	20	32	179	27
Yb_2O_3	9,2	0,6	350	1	100				

Although the radiation length of YAP is not small ($X_0=2.8$ cm), owing to the relatively low effective Z the Molière radius determining the transverse dimensions of the electron shower is fairly small ($R_M=2.8$; Ref. 5). In that study it was suggested that it may be possible to raise the crystal density ($d=5.36$ g/cm^2) by replacing the yttrium by ytterbium.

Fast, heavy scintillating materials

The properties of a series of such scintillators are given in Table VIII (Ref. 146). Most of them have three components of light emission, the contribution of which to the total light output I is given in percent. The value of I itself is given in relative units based on BGO, which is the heaviest of the scintillating crystals widely used at present.

The pure form of $PbCO_3$ unmixed with lead hydroxide has $I=9\%$ of the light output of BGO, but is an order of magnitude faster.[147] The very heavy Yb_2O_3 crystal is faster than plastic scintillators, but its light output is tiny. The crystals given in the table had small dimensions. $PbCl_2$ crystals are the least difficult to prepare, but they are also the lightest.

A series of heavy tetrafluorides such as Zn, Zr, Hf, and ThF_4, which can operate in large radiation fluxes, is attractive for electromagnetic calorimetry.[5] The luminescence time of, in particular, ThF_4 ($X_0=1.18$ cm) is less than 25 nsec, and its emission peaks are located at $\lambda=315$, 330, and 450 nm. LiYbF ($X_0=1.5$ cm) has the same luminescence time, and its emission lies in the visible range ($\lambda_{max}=450$ nm).

The crystal CdI_2 is interesting.[145] Its light output is 10% of the value for NaI(Tl), and its luminescence time is 3 nsec. The crystal density is 5.67 g/cm^3, and its radiation stability is $\sim 10^7$ rad.

Lutetium oxyorthosilicate $Lu_2(SiO_4)O$:Ce doped with cerium is similar to GSO:Ce in content.[148] Its characteristics are $d=7.4$ g/cm^2, $X_0=1.14$ cm, $n=1.82$, $\tau=40$ nsec, $\lambda=420$ nm, it is nonhygroscopic, and it has a large light output 75% compared with NaI(Tl). We see that the characteristics are very attractive. The sizes, as for all the other crystals described here, are still small.

The energy resolution at the 662-keV line measured using a LuSO:Ce crystal of dimensions $5\times5\times25$ mm was 12.4%. Intrinsic background of natural radioactivity at a rate of 200 counts per second was observed below 307 keV.

Paired sodium and bismuth tungstate

The Chokhral'skiĭ technique has been used to grow crystals of the type $NaBi(WO_4)_2$ of length 22 cm from a WO_3–B_2O_3–Na_2O mixture.[149] The former (NBW) has density 7.5 g/cm^3, $X_0=1.01$ cm, and $R_M=2$ cm.

Pure NBW does not scintillate and is interesting as a Čerenkov emitter with high density and large index of refraction $n=1.92$. A special advantage of it is its high radiation stability. The optical transmission of the crystal after irradiation with a 12-Mrad dose of γ rays from ^{60}Co at $\lambda=500$ nm falls by 30%. However, a 10-minute exposure of the crystal to ultraviolet light was sufficient to restore its original transmission. The crystal was prepared from relatively inexpensive raw material, and its melting temperature is relatively low (900 °C).

The hypothetical price of NBW is 2–3 US dollars per 1 cm^3. NBW has been doped with a dopant which, according to Ref. 140, scintillates at $\lambda_{max}=510$ nm with $\tau=3$ nsec. The light yield of this scintillator is more than 1% of the value for NaI(Tl). The radiation stability remained the same as for the Čerenkov emitter.

11. OTHER INORGANIC SCINTILLATING MONOCRYSTALS

In Figs. 24 and 25, where we give the values of the resolutions for various crystals, below the curves for BGO lie the curves for scintillating crystals of cadmium tungstate (CWO for short).[150,151] The efficiency of CWO in recording γ quanta is almost the same as that of BGO, and its light yield is as much as $0.4\eta_0$ [$\eta_0=1$ for NaI(Tl)]. However, it is much better than BGO in rate of response, having luminescence times $\tau_1=5$ μsec and $\tau_2=20$ μsec. As for BGO, the peak emission occurs at $\lambda=480$ nm and the afterglow is small. The unique property of CWO is the nearly complete independence of the light yield of temperature in the range 50–70 °C, where the temperature coeffi-

TABLE IX. (Ref. 163). Properties of GS1 scintillating glass.

Content by weight, %	
SiO_2	55
MgO	24
Al_2O_3	11
Li_2O	6
Cl_2O_3	4
Density, g/cm^3	2,64
Average index of refraction	1,586
Radiation length, cm	9,77
Nuclear interaction length, cm	37,4
dE/dx for particles with minimum ionization, MeV/cm	4,6
Number of photons/keV	1,5±0,5
Luminescence time of the fast component,* nsec	55
Wavelength for maximum emission, nm	395
Attenuation length, cm	20

*According to Ref. 167, the fast component makes up only 35% of the total light and its luminescence time is 74 nsec.

cient is only 0.01%/°C. Stability to the effects of climatic and mechanical factors is very important for using the crystal in geophysical and logging applications.

The radiation strength of CWO is close to that of BGO. The technology of obtaining high-transmission crystals of CWO is not yet well developed, which means that the dimensions are extremely limited (~25 mm).

Other scintillating tungstates of the alkali-earth metals Ca, Zn, Mo, and Co also come in small sizes and have long luminescence times. Of these, $CaWO_4$ stands out as having the maximum light yield ($0.5\eta_0$). Its luminescence components lie in the range 0.5–20 μsec. The maximum of the light-emission spectrum is located at 430 nm, which well matches the spectral sensitivity of a photodiode based on HgI_2. A resolution of 12.5% on a 662-keV line has been obtained by using this photodiode with a 10×10 mm crystal.[152]

$ZnWO_4$ has fairly high radiation stability; the parameters of a 1.5×1.5×1.5 mm crystal practically did not change after irradiation with a 5×10^5 rad dose from ^{60}Co (Ref. 153). This crystal luminesces with intensity $0.26\eta_0$ at $\lambda=490$ nm (Ref. 154). There are three luminescence components: $\tau_1=0.1$ μsec ($I_1=5\%$), $\tau_2=3.3$ μsec ($I_2=76\%$), and $\tau_3=20$ μsec ($I_3=19\%$).

The main area of application of tungstates is in computerized tomography.

In electron detection the problem arises of their reflection upon entering denser matter. This reflection is smaller, the lower the value of Z of the scintillator. The scintillating crystal CaF_2(Eu) is a good material in this regard. Its light yield reaches $0.5\eta_0$, the peak emission occurs at $\lambda=415$ nm, $\tau=0.95$ μsec, and the afterglow is small.[14] The energy resolution, as can be seen from Fig. 24, is moderate, the same as that of GSO:Ce. Most of the applications are for the detection of β and low-energy γ and x rays.

Another fluoride, CsF, is a very fast scintillator with peak emission at $\lambda=390$ nm. It has a luminescence time of 2.5 nsec (Ref. 69), $\eta=(0.03\text{–}0.06)\eta_0$, and $\eta=0.1\eta_0$ according to the data of Ref. 155. A time resolution of 150 psec in the coincidence of γ rays from ^{60}Co has been obtained for this crystal.[156] However, the use of the crystal is very limited, owing to its high hygroscopicity.

Another fast fluoride is the crystal $LaF_3(Nd^{3+})$, which has $\tau=6$ nsec (Ref. 157). Its peak emission occurs at $\lambda=173$ nm and exceeds the fast component of BaF_2 (Ref. 158). The crystal can be used in conjunction with a photosensitive proportional chamber.

The LiI(Eu) monocrystal is well known as an efficient neutron detector. Thermal neutrons interacting with ^{6}Li produce α particles with fixed energy 4.78 MeV and ^{3}H. Natural lithium contains 7.5% ^{6}Li, but lithium with enrichment by this isotope to 96% is also produced. The light yield of the crystal is $0.35\eta_0$, and the luminescence is 0.6 μsec for γ rays and 1.4 μsec for neutrons. The energy resolution for the α peak is usually 4–5%. A drawback of this crystal is its hygroscopicity.

The ZnSe(Te) and CdSe(Te) are known for the fact that they scintillate in the largest wavelength range, which is required for good matching to silicon photodiodes.[158] For example, for ZnSe(Te) $\lambda=640$ nm, $\eta=0.15\eta_0$, and $\tau=10$ μsec. A drawback of these crystals is their small transmission to their intrinsic radiation, which imposes a limit on their size. Their diode matching and small afterglow allow them to be used in tomography and dosimetry.

A remarkable property of the ZnSe(Te) crystal is the linearity of the light yield at large ionization density. For this crystal the α/β ratio is unity, and for a crystal of dimensions 10×7×5 mm the resolution for α particles of ^{241}Am was 13% (Ref. 160).

12. SCINTILLATING GLASSES

Elements such as terbium, cerium, and praseodymium scintillate. Glass activated with oxides of these elements becomes a scintillator.

Tb_2O_3 emits light at $\lambda_{max}=550$ nm, and its absorption and emission spectra are fairly well separated.[161] The luminescence time is ~ 3 msec. Tb_2O_3 has been used in wire x-ray detectors.[162]

Ce_2O_3 is faster. Its properties are listed in Table IX (Ref. 163). The distinctive feature of this scintillator is its high radiation stability. Even after irradiation by a dose of 10^8 rad the original characteristics can be completely restored by annealing at 400 °C (Ref. 164). Scintillating glass activated by Ce_2O_3 has become interesting in connection with the development of wire detectors for high-energy physics (Refs. 161, 165, and 166). However, significant afterglow has been observed in this glass after it is irradiated with a large dose. Glass activated with Pr^{3+} is even faster.[168] The components of the light emitted from them have a luminescence time of from 30 nsec to several microseconds. However, the light yield of glass containing Pr^{3+} is lower by a factor of two than that of glass containing Ce_2O_3. Scintillating glasses activated with terbium and then further addition of lithium for efficient neutron detection are studied in Ref. 169. In a wire detector made from such glass the light attenuation length was greater than 20 cm.

For electromagnetic calorimetry it is interesting to use fluoride glasses with radiation strength higher than that of other glasses.[5] Fluoride glasses activated with Ce^{3+} ions scintillate with $\tau=16$ nsec at $\lambda_{max}=320$ nm (for the type HFG 320, $d=5.75$ g/cm^3) and with $\tau=20$ nsec at $\lambda_{max}=320$ nm (for the type AFG 450, $d=5.75$ g/cm^3). An attractive feature of glasses is their low cost.

[1] J. B. Birks, *The Theory and Practice of Scintillation Counting* (Pergamon Press, London, 1964).
[2] Yu. K. Akimov, *Scintillation Counters in High Energy Physics* (Academic Press, New York, 1965) [Russian original, Moscow State University Press, Moscow, 1963).
[3] R. L. Heath, R. Hofstadter, and E. B. Hughes, Nucl. Instrum. Methods **162**, 431 (1979).
[4] Yu. A. Tsirlin, M. E. Globus, and E. P. Sysoeva, *Optimization of Detection of Gamma Radiation by Scintillating Crystals* [in Russian] (Énergoatomizdat, Moscow, 1991).
[5] P. Lecoq, M. Schussler, and M. Schneegans, Nucl. Instrum. Methods A **315**, 337 (1992).
[6] Particle Data Group, Phys. Lett. **239B**, 1116 (1990).
[7] D. E. Persyk and T. E. Moi, IEEE Trans. Nucl. Sci. **NS-29**, 615 (1978).
[8] A. M. Sandorfi and M. T. Collins, Nucl. Instrum. Methods **222**, 479 (1984).
[9] M. Jääskeläinen, D. G. Sarantites, R. Woodward *et al.*, Nucl. Instrum. Methods **204**, 385 (1983).
[10] M. Metag, in *Lecture Notes in Physics*, edited by W. V. Oertzen (Springer-Verlag, New York, 1983), Vol. 178, p. 163.
[11] R. Bass, W. Kessel, and G. Majoni, Nucl. Instrum. Methods **30**, 237 (1964).
[12] C. M. Bartle, Nucl. Instrum. Methods **124**, 547 (1975).
[13] L. M. Shamovskiĭ, *Crystallophosphors and Scintillators in Geology* [in Russian] (Nedra, Moscow, 1985).
[14] Harshaw Radiation Detector Filtrol Scintillation Phosphor Catalogue, 1984.
[15] H. Grassman, E. Lorenz, and H. G. Moser, Nucl. Instrum. Methods **228**, 323 (1985).
[16] E. Sakai, IEEE Trans. Nucl. Sci. **NS-34**, 418 (1987).
[17] E. Lorenz, IEEE Trans. Nucl. Sci. **NS-31**, 48 (1984).
[18] G. Blanar, H. Dietl, J. Dobbins *et al.*, Nucl. Instrum. Methods A **203**, 213 (1983).
[19] E. Blucher, B. Gittelman, B. K. Heltsley *et al.*, Nucl. Instrum. Methods A **249**, 201 (1986).
[20] H. Grassman, E. Lorenz, H. G. Moser *et al.*, Nucl. Instrum. Methods A **235**, 319 (1985).
[21] Crystal Barrel Collaboration, Nucl. Instrum. Methods A **321**, 69 (1992).
[22] M. Kobayashi, P. Carlson, and S. Berglund, Nucl. Instrum. Methods A **302**, 47 (1991).
[23] U. Kilgus, R. Kotthaus, and E. Lange, Nucl. Instrum. Methods A **297**, 425 (1990).
[24] V. K. Lyapidevskiĭ and V. A. Prorvich, Prib. Tekh. Exp. No. 2, 62 (1974); No. 5, 69 (1978) [Instrum. Exp. Tech.].
[25] S. Kubota, S. Sakuragi, S. Hashimotu *et al.*, Nucl. Instrum. Methods A **268**, 275 (1988).
[26] C. L. Woody, P. W. Levy, J. A. Kierstead *et al.*, IEEE Trans. Nucl. Sci. **NS-37**, 492 (1990).
[27] R. J. Meijer, A. Van den Brink, E. A. Bakkum *et al.*, Nucl. Instrum. Methods A **256**, 521 (1987).
[28] W. G. Gong, Y. D. Kim, G. Poggi *et al.*, Nucl. Instrum. Methods A **268**, 190 (1988).
[29] F. Benrachi, B. Chambon, B. Cheynis *et al.*, Nucl. Instrum. Methods A **281**, 137 (1989).
[30] C. J. W. Twenhofel, P. F. Box, P. Schotanus *et al.*, Nucl. Instrum. Methods B **51**, 58 (1990).
[31] J. Alarja, A. Dauchy, A. Giorni *et al.*, Nucl. Instrum. Methods A **242**, 352 (1986).
[32] P. Kreutz, A. Künmichel, C. Pinkenburg *et al.*, Nucl. Instrum. Methods A **260**, 120 (1987).
[33] Xi Hongfei, Zhang Wenlong, Guo Zhon Gyan *et al.*, Nucl. Instrum. Methods A **320**, 504 (1992).
[34] F. A. Agaronyan, A. G. Akhierdzhanyan, M. Gonusek *et al.*, Report R13-87-15, JINR, Dubna (1987) [in Russian].
[35] G. Viesti, G. Prete, D. Fabris *et al.*, Nucl. Instrum. Methods A **252**, 75 (1986).
[36] E. Valtonen, J. Peltonen, and J. J. Torsti, Nucl. Instrum. Methods A **286**, 169 (1990).
[37] D. Horn, G. C. Ball, A. Galindo-Uribarri *et al.*, Nucl. Instrum. Methods A **320**, 273 (1992).
[38] B. K. Utts and S. E. Spagno, IEEE Trans. Nucl. Sci. **NS-37**, 134 (1990).
[39] P. Schotanus, R. Kamermans, and P. Dorenbos, *ibid.*, p. 177.
[40] S. Keszthelyi-Landori, I. Földvàri, R. Voszka *et al.*, Nucl. Instrum. Methods A **303**, 374 (1991).
[41] A. V. Gektin, A. I. Gorelov, V. I. Rykalin *et al.*, Nucl. Instrum. Methods A **294**, 591 (1991).
[42] M. I. Weber and R. R. Monchamp, J. Appl. Phys. **44**, 5496 (1983).
[43] O. H. Nestor and C. Y. Huang, IEEE Trans. Nucl. Sci. **NS-22**, 68 (1975).
[44] M. H. Murashita, H. Saitoh, K. Tobimatsu *et al.*, Nucl. Instrum. Methods A **243**, 67 (1986).
[45] L3 Collaboration, Nucl. Instrum. Methods A **289**, 35 (1990).
[46] M. R. Farukhi, in *Proc. of the Symp. on Nuclear Radiation Detector Materials*, Massachusetts, 1982, p. 115.
[47] C. L. Melcher, R. A. Manenta, and J. S. Schweitzer, IEEE Trans. Nucl. Sci. **NS-36**, 1188 (1989).
[48] R. D. Ransome, V. R. Cupps, S. Danson *et al.*, Phys. Rev. Lett. **64**, 372 (1990); Phys. Rev. C **42**, 1500 (1990).
[49] A. Zucchiatti, P. Levi Sandri, C. Scherf *et al.*, Nucl. Instrum. Methods A **321**, 219 (1992).
[50] A. E. Evans, Jr., IEEE Trans. Nucl. Sci. **NS-27**, 172 (1980).
[51] D. M. Drake, L. R. Nilsson, and J. Fancett, Nucl. Instrum. Methods **188**, 313 (1981).
[52] O. Hausser, M. A. Lone, T. K. Alexander *et al.*, Nucl. Instrum. Methods **213**, 301 (1983).
[53] R. R. Kiziah and S. R. Lowell, Nucl. Instrum. Methods A **305**, 129 (1991).
[54] P. Corvisiero, M. Anghinolfi, L. Z. Dzhilavyan *et al.*, Nucl. Instrum. Methods A **294**, 478 (1990).
[55] N. Zhang, Z. Ding, Y. Wu, and M. Solomon, IEEE Trans. Nucl. Sci. **NS-37**, 216 (1990).

[56] A. Zucchiatti, M. Castoldi, G. Gervino *et al.*, Nucl. Instrum. Methods A **317**, 492 (1992).
[57] H. Dietl, J. Dobbins, E. Lorenz *et al.*, Nucl. Instrum. Methods A **235**, 464 (1985).
[58] R. D. Schamberger, U. Heintz, J. Lee-Franzini *et al.*, Nucl. Instrum. Methods A **309**, 450 (1991).
[59] M. Anghinolfi, M. Castoldi, P. Corvisiero *et al.*, Nucl. Instrum. Methods A **317**, 531 (1992).
[60] R. Sumner, Nucl. Instrum. Methods A **265**, 252 (1988).
[61] Ren-yuan Zhu, Nucl. Instrum. Methods A **306**, 145 (1991).
[62] G. Gervino, M. Anghinolfi, M. Castoldi *et al.*, Nucl. Instrum. Methods A **309**, 497 (1991).
[63] M. R. Farukhi and C. F. Swinehart, IEEE Trans. Nucl. Sci. **NS-18**, 200 (1971).
[64] L. Laval, M. Moszynski, R. Allemand *et al.*, Nucl. Instrum. Methods **206**, 169 (1983).
[65] P. Schotanus, C. W. E. van Eijk, R. W. Hollander *et al.*, IEEE Trans. Nucl. Sci. **NS-34**, 272 (1987).
[66] C. L. Woody, P. W. Levy, and J. A. Kierstead, IEEE Trans. Nucl. Sci. **NS-36**, 536 (1986).
[67] G. Crahan and H. Yamamoto, Nucl. Instrum. Methods A **307**, 240 (1991).
[68] M. H. Murashita, H. Saitoh, K. Tobimatsu *et al.*, Nucl. Instrum. Methods A **243**, 67 (1986).
[69] E. J. Hoffmann, M. Dahebom, and A. R. Ricci, IEEE Trans. Nucl. Sci. **NS-33**, 420 (1986).
[70] D. F. Anderson and D. C. Lamb, Nucl. Instrum. Methods A **260**, 377 (1987).
[71] P. Sperr, Nucl. Instrum. Methods A **254**, 635 (1987).
[72] W. Klarma, Th. Lindblad, M. Moszynski *et al.*, Nucl. Instrum. Methods A **254**, 85 (1987).
[73] K. Wisshak and F. Käppeler, Nucl. Instrum. Methods **227**, 91 (1984).
[74] V. V. Yanovskiĭ, Ya. A. Valbis, and P. Kozma, Preprint LIYaF-1499, Leningrad Nuclear Physics Institute, Gatchina (1989).
[75] W. Karle, M. Knopp, K.-H. Speidel *et al.*, Nucl. Instrum. Methods A **271**, 571 (1988).
[76] K. Wisshak, F. Käppeler, and K. Gubber, IEEE Trans. Nucl. Sci. **NS-36**, 101 (1989).
[77] K. Wisshak, F. Käppeler, and H. Muller, Nucl. Instrum. Methods A **251**, 101 (1986).
[78] K. Wisshak, K. Gubber, and F. Käppeler, Nucl. Instrum. Methods A **259**, 583 (1987).
[79] H. Kobayashi, A. Konaka, K. Miyake *et al.*, Nucl. Instrum. Methods A **270**, 106 (1988).
[80] P. Shotanus, C. W. E. van Eijk, R. W. Hollander *et al.*, Nucl. Instrum. Methods A **238**, 554 (1985).
[81] P. Mine, J. C. Santiard, D. Scigocki *et al.*, IEEE Trans. Nucl. Sci. **NS-34**, 458 (1987).
[82] R. Bouclier, G. Charpak, W. Gao *et al.*, Nucl. Instrum. Methods A **267**, 69 (1988).
[83] A. Zichichi, "The LAA Project," CERN-LAA/88-2, CERN, Geneva (1988).
[84] I. Giomataris and G. Charpak, Preprint CERN-EP/88-94, CERN, Geneva (1988).
[85] D. F. Anderson, R. Bouchlier, G. Charpak *et al.*, Nucl. Instrum. Methods **217**, 217 (1983).
[86] K. Tailor, O. M. Nestor, and B. Utts, IEEE Trans. Nucl. Sci. **NS-33**, 243 (1986).
[87] P. Shotanus, P. Dorenbos, C. W. E. van Eijk *et al.*, IEEE Trans. Nucl. Sci. **NS-36**, 132 (1989).
[88] Hamamatsu Photonics KK, Ichinocho, Hamamatsu 435, Japan.
[89] Ren-yuan Zhu, in *Proc. of the Symp. on Detector Research and Development for the SSC*, Fort Worth, Texas, 1990, p. 340.
[90] T. Matulewicz, E. Grosse, H. Emling *et al.*, Nucl. Instrum. Methods A **289**, 194 (1990).
[91] J. Geihl, D. Hauff, J. M. Henneberg *et al.*, Nucl. Instrum. Methods A **263**, 392 (1988).
[92] E. Lorenz, G. Mageras, and H. Vogel, Nucl. Instrum. Methods **249**, 235 (1986).
[93] J. Clayton, W. Benenson, N. Levinsky *et al.*, Nucl. Instrum. Methods A **305**, 116 (1991).
[94] A. Badala, R. Barbera, A. Palmeri *et al.*, Nucl. Instrum. Methods A **306**, 283 (1991).
[95] E. Migneco, C. Agodi, R. Alba *et al.*, Nucl. Instrum. Methods A **314**, 31 (1992).
[96] S. Kubota, M. Suzuki, Jian-zhi Ruan (Gen) *et al.*, Nucl. Instrum. Methods A **242**, 291 (1986).
[97] E. Dafni, Nucl. Instrum. Methods A **254**, 54 (1987).
[98] T. Murakami, J. Kasagi, H. Tachibanaki *et al.*, Nucl. Instrum. Methods A **253**, 163 (1986).
[99] C. Agodi, R. Alba, G. Bellia *et al.*, Nucl. Instrum. Methods A **269**, 595 (1986).
[100] R. Novotny, R. Riess, R. Hingmann *et al.*, Nucl. Instrum. Methods A **252**, 340 (1987).
[101] G. Lanzanò, A. Pagano, S. Urso *et al.*, Nucl. Instrum. Methods A **312**, 515 (1992).
[102] W. Klarma, Th. Lindbland, M. Moszynski *et al.*, Nucl. Instrum. Methods A **265**, 485 (1988).
[103] V. Yanovsky and P. Kozma, Nucl. Instrum. Methods A **276**, 659 (1989).
[104] P. Kozma and V. Yanovsky, Nucl. Instrum. Methods A **281**, 346 (1989).
[105] L. Sh. Afanasiadi, Ya. A. Vilbas, N. Z. Galtskov *et al.*, Prib. Tekh. Eksp. No. 1, 77 (1989) [Instrum. Exp. Tech.].
[106] T. Shimizu, S. Kubota, T. Motobayashi *et al.*, IEEE Trans. Nucl. Sci. **NS-34**, 370 (1986).
[107] S. Kubota, T. Motobayashi, Jian-zhi Ruan (Gen) *et al.*, IEEE Trans. Nucl. Sci. **NS-34**, 438 (1987).
[108] D. R. Winn and M. Whitmore, IEEE Trans. Nucl. Sci. **NS-36**, 256 (1989).
[109] Yu. A. Tsirlin, E. L. Vinograd, N. Yu. Gurevich *et al.*, At. Energ. **45**, 69 (1978) [in Russian].
[110] E. L. Vinograd, N. Yu. Gurevich, and Yu. A. Tsirlin, At. Energ. **48**, 335 (1980) [in Russian].
[111] G. J. Bobbink, A. Engler, R. W. Kraemer *et al.*, Nucl. Instrum. Methods **227**, 470 (1984).
[112] Ch. Bieler, D. Burkart, J. Marks *et al.*, Nucl. Instrum. Methods A **234**, 435 (1985).
[113] S. Schlögl, H. Spitzer, and K. Wittenburg, Nucl. Instrum. Methods A **242**, 89 (1985).
[114] M. Kobayashi and S. Sakuragi, Nucl. Instrum. Methods A **254**, 275 (1987).
[115] C. L. Melcher, IEEE Trans. Nucl. Sci. **NS-32**, 545 (1985).
[116] M. Kobayashi, K. Kondo, H. Hirabayashi *et al.*, Nucl. Instrum. Methods **206**, 107 (1983).
[117] A. J. Caffrey, R. L. Heath, P. D. Ritter *et al.*, IEEE Trans. Nucl. Sci. **NS-33**, 230 (1986).
[118] C. Laviron and P. Lecoq, Nucl. Instrum. Methods **227**, 45 (1984).
[119] R. Y. Zhu, H. Stone, H. Newman *et al.*, Nucl. Instrum. Methods A **302**, 69 (1991).
[120] P. Lecoq, P. J. Liand, B. Rostaing *et al.*, Nucl. Instrum. Methods A **300**, 240 (1991).
[121] Z. W. Yin, Z. Y. Wei, D. Z. Shen, and Y. Y. Xie, Nucl. Instrum. Methods A **275**, 273 (1989).
[122] A. C. Rester, G. S. Bamford, R. L. Coldwell *et al.*, Nucl. Instrum. Methods A **297**, 258 (1990).
[123] S. Majewski and D. Anderson, Nucl. Instrum. Methods A **241**, 76 (1985).
[124] S. Majewski and M. K. Bentley, Nucl. Instrum. Methods A **260**, 373 (1987).
[125] A. Murakami, H. Asakura, and H. Yoshinaka, Nucl. Instrum. Methods A **301**, 435 (1991).
[126] M. Kobayashi, S. Ishimoto, S. Sugimoto *et al.*, Nucl. Instrum. Methods A **305**, 401 (1991).
[127] D. F. Anderson, IEEE Trans. Nucl. Sci. **NS-36**, 137 (1989).
[128] W. W. Moses and S. E. Derenzo, *ibid.*, p. 173.
[129] D. F. Anderson, Nucl. Instrum. Methods A **287**, 606 (1990).
[130] M. Kobayashi, M. Ishii, E. A. Krivandina *et al.*, Nucl. Instrum. Methods A **302**, 443 (1991).
[131] K. Takagi and T. Fukazawa, Appl. Phys. Lett. **42**, 43 (1983).
[132] H. Ishibashi, K. Shimizu, K. Susa *et al.*, IEEE Trans. Nucl. Sci. **NS-36**, 170 (1989).
[133] C. L. Melcher, J. Schweitzer, T. Utsu *et al.*, IEEE Trans. Nucl. Sci. **NS-37**, 161 (1990).
[134] M. Kobayashi, K. Takamatsu, S. Ide *et al.*, Nucl. Instrum. Methods A **306**, 139 (1991).

[135] E. Gramsch, K. G. Lynn, M. Weber *et al.*, Nucl. Instrum. Methods A **311**, 529 (1992).
[136] V. V. Kamanin, A. Kugler, Yu. É. Penionzhkevich *et al.*, Fiz. Elem. Chastits At. Yadra **20**, 741 (1989) [Sov. J. Part. Nucl. **20**, 311 (1989)].
[137] N. Alamanos, B. Braun-Munzinger, R. F. Freifelder *et al.*, Phys. Lett. **173B**, 392 (1986).
[138] V. V. Yanovsky, V. A. Chizov, and V. M. Skorikov, Nucl. Instrum. Methods A **309**, 596 (1991).
[139] E. G. Gumanskaya, B. I. Zadneprovskiĭ, M. V. Korzhik *et al.*, Zh. Prikl. Spektrosk. **56**, 302 (1992) [in Russian].
[140] B. I. Zadneprovskiĭ, private communication.
[141] A. A. Aseev, E. G. Devitsin, V. A. Kozlov *et al.*, Nucl. Instrum. Methods A **313**, 340 (1992).
[142] R. Autrata and P. Schaner, J. Phys. Eng. **4**, 707 (1978); Scanning **5**, 91 (1983).
[143] V. G. Baryshevskiĭ, M. V. Korzhik, V. I. Moroz *et al.*, Prib. Tekh. Eksp. No. 3, 86 (1992) [Instrum. Exp. Tech.].
[144] V. A. Kachanov, V. I. Rykalin, V. L. Solovyanov *et al.*, Nucl. Instrum. Methods A **314**, 215 (1992).
[145] G. I. Britvich, A. I. Peresypkin, V. G. Vasil'chenko *et al.*, Nucl. Instrum. Methods A **308**, 509 (1991).
[146] S. E. Derenzo, W. W. Moses, J. L. Cahoon *et al.*, IEEE Trans. Nucl. Sci. **NS-37**, 203 (1990).
[147] W. W. Moses and S. E. Derenzo, *ibid.*, p. 96.
[148] C. L. Melcher and J. S. Schweitzer, Nucl. Instrum. Methods A **314**, 212 (1992).
[149] V. A. Nephyodov, D. I. Zadneprovsky, P. V. Nephyodov *et al.*, Report presented at the Intern. Workshop LUMDETR '91, Riga, October, 1991.
[150] M. R. Farukhi, IEEE Trans. Nucl. Sci. **NS-29**, 1237 (1982).
[151] C. L. Melcher, R. A. Manete, and J. S. Schweitzer, IEEE Trans. Nucl. Sci. **NS-36**, 1188 (1989).
[152] J. Markakis, C. Ortale, and W. Schnepple, IEEE Trans. Nucl. Sci. **NS-32**, 559 (1985).
[153] Ya. A. Balbis, Z. A. Rachko, and Yu. A. Yansons, Opt. Spektrosk. **64**, 1196 (1988) [Opt. Spectrosc. (USSR) **64**, 714 (1988)].
[154] H. Grassman, H. G. Moser, and E. Lorenz, J. Lumin. **33**, 109 (1985).
[155] M. Moszynski, R. Allemand, M. Laval *et al.*, Nucl. Instrum. Methods **205**, 239 (1983).
[156] V. Yanovsky and P. Kozma, Nucl. Instrum. Methods A **276**, 659 (1989).
[157] P. Dorenbos, C. W. E. van Eijk, R. W. Hollander *et al.*, IEEE Trans. Nucl. Sci. **NS-37**, 119 (1990).
[158] M. Gruwè and S. Tavernier, Nucl. Instrum. Methods A **311**, 301 (1992).
[159] V. D. Ryzhikov, P. E. Stadnik, and Yu. A. Yakovlev, Prib. Tekh. Eksp. No. 5, 6 (1984) [Instrum. Exp. Tech.].
[160] F. A. Danevich, Yu. T. Zdesenko, A. S. Nikolaĭko *et al.*, Prib. Tekh. Eksp. No. 5, 80 (1989) [Instrum. Exp. Tech.].
[161] R. Ruchti, B. Baumbaugh, J. Bishop *et al.*, IEEE Trans. Nucl. Sci. **NS-31**, 69 (1984).
[162] H. Shao, D. W. Miller, and C. R. Pearsall, Nucl. Instrum. Methods A **299**, 528 (1990).
[163] J. Kirkby, Preprint CERN-EP/87-60, CERN, Geneva (1987).
[164] M. Atkinson, J. Fent, C. Fisher *et al.*, Nucl. Instrum. Methods A **254**, 500 (1987).
[165] R. Ruchti, B. Bambaugh, J. Bishop *et al.*, IEEE Trans. Nucl. Sci. **NS-33**, 151 (1986).
[166] C. Angelini, W. Beusch, I. J. Bloodworth *et al.*, Nucl. Instrum. Methods A **277**, 132 (1989).
[167] C. Angelini, W. Beusch, D. J. Crennell *et al.*, Nucl. Instrum. Methods A **281**, 50 (1989).
[168] A. Rogers, B. Kinchen, B. Bambaugh *et al.*, IEEE Trans. Nucl. Sci. **NS-34**, 541 (1987).
[169] G. B. Spector, T. McCollum, and A. R. Spowart, Nucl. Instrum. Methods A **313**, 373 (1992).
[170] K. M. James, M. Y. Masterson, and R. Farrel, Nucl. Instrum. Methods A **313**, 196 (1992).

Translated by Patricia A. Millard